Received: 18 December 2020 | Revised: 15 January 2021 | Accepted: 15 January 2021

DOI: 10.1002/pol.20200862

REVIEW

JOURNAL OF POLYMER SCIENCE WILEY

Properties and applications of precision oligomer materials; where organic and polymer chemistry join forces

Bas van Genabeek[1,2] | **Brigitte A. G. Lamers**[1,2] | **Craig J. Hawker**[3,4] | **E. W. Meijer**[1,2] | **Will R. Gutekunst**[5] | **Bernhard V. K. J. Schmidt**[6,7]

[1]Laboratory of Macromolecular and Organic Chemistry, Eindhoven University of Technology, Eindhoven, The Netherlands

[2]Institute for Complex Molecular Systems, Eindhoven University of Technology, Eindhoven, The Netherlands

[3]Materials Research Laboratory, University of California, Santa Barbara, California

[4]Materials Department, University of California, Santa Barbara, California

[5]School of Chemistry and Biochemistry, Georgia Institute of Technology, Atlanta, Georgia

[6]Department of Colloid Chemistry, Max Planck Institute of Colloids and Interfaces, Potsdam, Germany

[7]School of Chemisty, University of Glasgow, Glasgow, UK

Correspondence
Bernhard V. K. J. Schmidt, School of Chemistry, University of Glasgow, G128QQ Glasgow, UK.
Email: bernhard.schmidt@glasgow.ac.uk

Will R. Gutekunst, School of Chemistry and Biochemistry, Georgia Institute of Technology, Atlanta, Georgia, USA
Email: willgute@gatech.edu

Abstract

Precise oligomeric materials constitute a growing area of research with implications for various applications as well as fundamental studies. Notably, this field of science which can be termed macro-organic chemistry, draws inspiration from both traditional polymer chemistry and organic synthesis, combining the molecular precision of organic chemistry with the materials properties of macromolecules. Discrete oligomers enable access to unprecedented materials properties, for example, in self-assembled structures, crystallization, or optical properties. The degree of control over oligomer structures resembles many biological systems and enables the design of materials with tailored properties and the development of fundamental structure–property relationships. This Review highlights recent developments in macro-organic chemistry from synthetic concepts to materials properties, with a focus on self-assembly and molecular recognition. Finally, an outlook for future research directions is provided.

KEYWORDS

discrete oligomers, macro-organic chemistry, oligomer materials, oligomers

This article is dedicated to Prof. François Diederich in commemoration of his contribution to chemical science.

Bas van Genabeek and Brigitte A. G. Lamers contributed equally to this Review.

Oligomer and macro-organic chemistry: Situated in between polymer chemistry and organic chemistry macro-organic chemistry combines the molecular precision of organic chemistry with materials properties of polymers, which offers exciting potential for the future. This Review highlights the developments in macro-organic chemistry from synthetic concepts to materials properties, with a focus on self-assembly and molecular recognition.

Funding information
Georgia Institute of Technology; Max-Planck-Gesellschaft; Ministerie van Onderwijs, Cultuur en Wetenschap, Grant/Award Number: Gravity program 024.001.035; Royal Netherlands Academy of Arts and Science; U.S. Army Research Office, Grant/Award Number: W911NF-19-2-0026; University of Glasgow

1 | INTRODUCTION AND SCOPE

Oligomers are comprised of repeating subunits that occupy a unique area of chemical space between discrete small molecules and higher molecular weight polymers. As a result, this emerging class of materials encompasses research opportunities from both categories, and frequently presents entirely new directions not present in either traditional class. While the transition from an oligomer to a polymer is not always clear from a purely structural point of view, the IUPAC definition describes an oligomer as a molecule that "has properties which do vary significantly with the removal of one or a few of the units," and the term will be used accordingly in this review.[1] This definition highlights a key driver for oligomer research, particularly in molecularly defined cases that has been a focus of materials scientists. What is the correlation between minor changes in oligomer structure which lead to significant changes and tunability in physical properties? This chemical space between classical organic and macromolecular chemistry we term "macro-organic chemistry" as it leverages the benefits from the advanced chemistry of both small molecules and polymers. This is exemplified by the importance of oligomer sequence and/or length in biological systems with classical examples being the interaction of oligosaccharides with lectins, the ability of siRNA to silence genes, or the loss of enzyme activity after a point mutation.[2] While the role of discrete oligomeric molecules continues to be an increasingly active area of research in (chemical) biology, the potential of abiotic synthetic oligomers to generate emergent thermal, mechanical, and self-assembly properties is significant. In these research fields, structural precision is crucial to arrive at novel properties or to fully understand the structure–property relationships of these more complex architectures.

From a historical point of view, the synthesis of biologically relevant oligomers brought organic and biochemists together in their efforts to push the frontiers on what is technically possible. Modern molecular biology would not exist without the groundbreaking synthesis of discrete and sequence-controlled oligopeptides, oligonucleotides, and oligosaccharides. It was not until the early 1980's that synthetic chemists combined advanced organic methodologies for the synthesis of complex liquid crystals, dendritic macromolecules, foldamers, and a large variety of π-conjugated oligomers and polymers.[3–10]

The present review highlights the different chemical approaches to precision oligomeric materials with a focus on materials properties that are modulated by a change in oligomer length, sequence, or stereochemistry.[11–13] Furthermore, given the breadth of chemical space that can be considered "oligomeric," this review will emphasize abiotic oligomeric species that have been recently developed for materials science applications and provide insights into structure–property relationships. A focus is placed on "precision" oligomers that are uniform in terms of length, sequence, and/or composition and their materials properties, especially in the context of traditional polymer features. Topics pertaining to oligopeptides,[14,15] oligonucleotides,[16,17] and oligosaccharides[18] for applications in the biomedical field will not be discussed, as these have already been thoroughly reviewed. Additionally, the field of dendrimer research has been reviewed in the past and will also not be described here, though many of the concepts illustrated by precision oligomeric materials also apply to dendrimers.[19–21] Similarly, readers are directed to pivotal reviews that examined the synthesis and properties of oligomeric surfactants,[22–24] where the assembly profile for these precision materials is exceedingly rich, and discrete π-conjugated oligomers.[25–27] The landmark review of Martin and Diederich in the Angewandte Chemie 1999 entitled "*Linear Monodisperse p-Conjugated Oligomers: Model Compounds for Polymers and More*" provides an excellent introduction[25] to this growing area.[28,29]

2 | SYNTHETIC APPROACHES TO DEFINED OLIGOMERS

The synthetic approaches used to prepare oligomers[17–23] have taken inspiration from both macromolecular chemistry and small molecule organic chemistry. At one extreme, classical synthetic polymer chemistry leads to structures with a distribution of molecular weights or degrees of polymerization (DP) and despite progress in controlled

and living polymerization, ensemble properties can be dominated by either low molecular weight or high molecular weight fractions. Moreover, the stereo-irregularity in many polymers results in no two molecules being structurally identical, for example a 1 kg sample of PMMA with a molecular weight of 20,000 Da (DP $\sim$ 200) leads statistically to all molecules having a different tacticity along the backbone and different degree of polymerization. In contrast, synthetic organic chemistry gives access to precise molecular entities with a single molecular weight ($Đ = 1$) and feature tunable, discrete properties, that are not governed by chain entanglement at lengths below the chain entanglement threshold.

Due to the prospect of utilizing precision oligomeric species that have emergent materials properties, a variety of synthetic strategies have been developed based on oligomer structure, size, and scale requirements. As not a single solution to this problem exists, the strategy employed changes with the desired goal, whether to explore new chemical space for an ideal sequence or for targeted and scalable materials production. These approaches to precise oligomers can be divided into two general strategies involving either iterative, multi-step syntheses or the separation of disperse oligomeric mixtures.

2.1 | Defined oligomers via iterative synthesis

Iterative synthesis of oligomers involves the sequential introduction of each monomer unit through individual chemical steps and can be categorized into two distinct growth modes: linear – either monodirectional or bidirectional – or exponential (Figure 1). These strategies permit the highest level of control of the oligomer sequence and provide substantial flexibility in design for identifying optimal materials properties.[11,13,30] In terms of time and efficiency, the development of automation has significantly impacted both approaches.

2.1.1 | Linear growth

Linear monodirectional growth strategies are used for macro-organic synthesis in solution-phase synthesis or solid-supported synthesis, and share many of the advantages and disadvantages encountered in oligopeptide synthesis. While utilization of solid phase supports allows convenient purification and isolation of the multi-step products, it can limit the quantity of oligomer produced

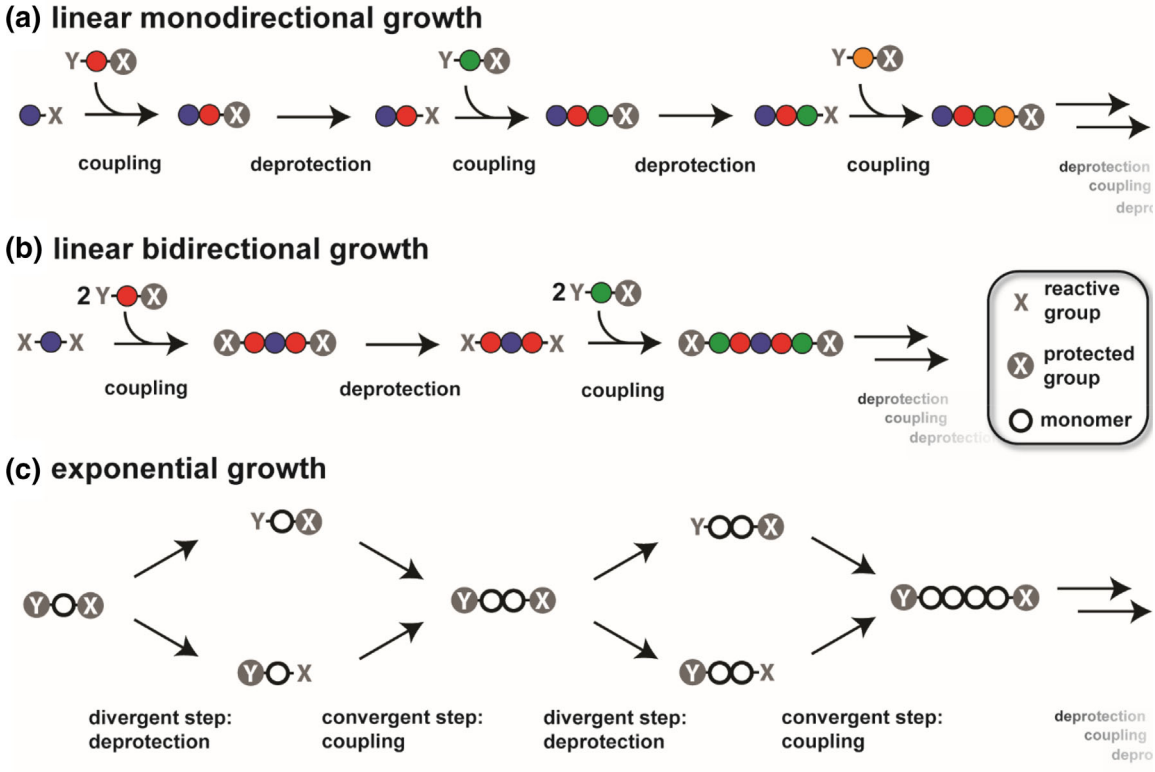

FIGURE 1 (a and b) Linear growth strategy based on sequential coupling of building blocks at one (a) or both sides (b) of the growing chain, and activation or deprotection to restore the reactive end-group; (c) exponential growth strategy or divergent/convergent approach based on the selective activation or deprotection of bifunctional molecules. Adapted with permission.[13] Copyright 2017, John Wiley and Sons 2017

due to the mass of the support. In contrast, solution-based syntheses are more challenging with respect to purification but higher concentrations can be achieved, leading to increased scale for the oligomeric product.[31] Clever solutions to overcome the disadvantages of the solid supports have been developed through the combination of polymer-supported solution phase chemistry and fluorous tags.[32] This permits the synthesis to be performed under homogeneous conditions, while the desired product sequence can easily be removed from excess reagents via simple precipitation/filtration through a fluorous solid-phase extraction, respectively.[33] Future opportunities exist to resolve these issues through the combination of solution and solid phase synthesis, as has been shown in the large scale, multi-ton production of the 36-amino-acid peptide therapeutic enfuvirtide.[34]

While iterative syntheses based on solid-phase supports have been widely used in the realm of oligonucleotide and oligopeptide synthesis, adaptation of these powerful methods to generate unnatural polypeptide and hybrid materials is gaining traction. Central to the success of these strategies is robust chemistry that can deliver very high, if not quantitative, yields of products. Lutz and coworkers exploited automated solid-phase synthesis to generate sequence encoded oligo(alkoxamine amide)s with DPs up to 24 units (Figure 2).[35] A second strategy employing highly robust phosphoramidite chemistry was used to create libraries of oligomers with significantly higher numbers of repeat units (Figure 2).[36,37] While large excesses of monomers (10 eq) were required, ultimately, milligram quantities of a 104-mer could be obtained in high purity. A related approach based on copper azide-alkyne cycloaddition (CuAAc) by Lutz and coworkers could be used to significantly expand the diversity of precise oligomeric structures with fine control over monomer sequence being demonstrated.[38–40] In these examples, oligomers were grown from a Wang-resin via consecutive amide formation and CuAAc without the utilization of protection group chemistry leading to the introduction of aliphatic, oligo ethylene glycols (oEGs), and amino acid units. This solid support strategy has also been utilized to prepare oligo(ethylene imines) up to 20 repeating units[41] with Du Prez and coworkers further illustrating the synthesis of sequence defined discrete oligomers based on thiolactone chemistry[42] and Börner and coworkers reporting the synthesis of PEGylated sequence defined oligomers.[43] Niu and coworkers described oligomer synthesis based on orthogonal CuAAc and sulfur–fluoride exchange reaction (SuFEx).[44] Iterative coupling via solid-support was investigated without utilization of protecting group chemistry. An interesting utilization of efficient carbonyldiimidazole coupling chemistry was performed by Anderson and coworkers during the synthesis of oligo(hydroxyproline).[45] Significantly, no protection-deprotection chemistry was needed for the formation of oligomers up to the hexamer with six differently functionalized prolines being utilized for sequence control.

To address scale limitations, linear strategies for the preparation of abiotic oligomers by solution-phase synthesis are rapidly being developed to deliver large materials libraries with highly optimized coupling chemistry. In this approach, oEG has been a central area of development due to the widespread application of PEG in numerous technologies. The work of Springer used benzyl protected and tosylated oEG building blocks to ultimately give PEG 29-mers that could be further functionalized with small peptide sequences.[46] Perhaps the most impressive example is an efficient and scalable route published by Jiang and coworkers where large amounts (>100 g) of macrocyclic oEG sulfate building

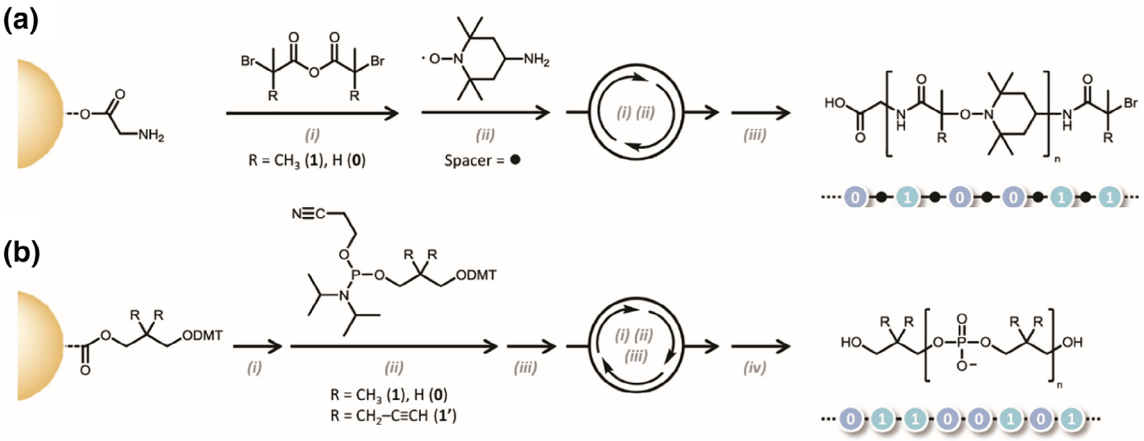

FIGURE 2 Strategies for obtaining sequence encoded oligomers by iterative solid-phase chemistry, using: (a) successive anhydride–amine and nitroxide radical coupling steps (adapted from Reference 35 licensed under CC-BY); (b) phosphoramidite chemistry. Reprinted with permission.[36,37] Copyright 2015, American Chemical Society

blocks were prepared from small linear oEG starting materials.[47,48] Subsequently, this macrocyclic building block was reacted with a broad selection of nucleophiles to give functional ring-opened products. Repetitive macrocyclization and ring-opening with a small oEG diol allowed the fabrication of even longer oligomers, containing up to 36 repeat units.

Recently, multicomponent reactions in solution have been explored by Meier and coworkers.[49] Uniform and sequence-defined oligomers were generated via the Passerini three-component and the Ugi four-component reaction in combination with subsequent thiol-ene addition. Through this process, molecular complexity can be enhanced in considerably fewer steps when compared to traditional iterative processes as a result of the highly convergent approach. After five Ugi steps, total yields of ~15% were achieved, corresponding to ~70% yield per step. Li and coworkers have also utilized the Passerini three component reaction to synthesize well-defined oligomers.[50] The different reactivities of aromatic and aliphatic nitriles was leveraged to allow chain extension without the need of protecting groups or a separate activating reaction. In an interesting orthogonal adaption, the Passerini reaction was combined with a photo-activated Diels–Alder coupling by Barner-Kowollik and coworkers.[51] In this approach, a bismaleimide functional central core was synthesized via Passerini reaction and subsequently conjugated with benzaldehyde derivatives via photoenolization to yield ABA type oligomers. Through the utilization of protected maleimides, higher-order oligomers could be prepared with a high degree of structural tolerance. A protection group-free strategy was subsequently developed by Gao and coworkers, who utilized CuAAc and the Menschutkin reaction for sequence defined oligomers with up to 12 repeating units.[52] The authors employed a polar-inverse strategy with a dramatic polarity difference between feed and product molecules that enabled a simple precipitation step for the purification of product from the individual addition steps.

Traditional linear polymers prepared through radical processes inherently result in products with a wide range of chain lengths. However, by clever selection of catalysts and monomers, Boyer and coworkers have developed a range of impressive strategies that permit individual monomer unit insertion under photochemically-mediated radical conditions.[53] Key to the efficiency of this process and to the purity of the resulting oligomeric products is the selection of chain transfer agents/monomer pairs. When *fac*-Ir(ppy)$_3$ and zinc tetraphenylporphyrin were utilized as photoredox catalysts together with trithiocarbonate-based chain transfer agents, monomers with low propagation rate, such as electron rich styrenics, functionalized maleimides, limonene, or vinyl acetate, could be used to achieve three sequential insertion steps with isolated yields of ~95% per step. Wavelength-specific insertion could also be achieved by using a green light source to form sequence controlled discrete oligomers via selective activation of the RAFT chain end.[54] After irradiation, the RAFT group could be aminolyzed and exchanged with a new RAFT agent to continue the single monomer insertion process. While the control over a normally stochastic process is impressive, the scope of this strategy is limited to specific monomer sets with significant future opportunities existing.

Linear growth strategies have also been developed in conjugated oligomer synthesis by Meyer and coworkers for the preparation of heterotelechelic oligo(para-phenylene vinylene) (oPPV).[55] This approach uses Grubbs cross-metathesis chemistry to introduce a benzaldehyde group to the terminus, which is transformed into a styrene-functionality for further extension through a Wittig reaction. Critical to this approach are the steric parameters of the coupling partners. By alternating substituted and unsubstituted aryl groups, a sequence-defined pentameric oPPV was prepared where the generated internal olefins are inert to the cross-metathesis chemistry. Given the flexibility in the chain end chemistry obtainable with this approach, the oligomers with terminal olefins at each terminus could be further polymerized using acyclic diene metathesis polymerization. Seferos and coworkers synthesized discrete oligo(3-hexyl thiophene) (o3HT) containing up to 18 units.[56] A stepwise catalyst transfer polymerization was employed to form oligomers in a homogenous one-pot approach using temperature cycling to control the elementary steps of the reaction. First, the bromothiophene monomer was deprotonated with lithium diisopropylamide in the presence of a nickel catalyst at low temperatures to generate a kinetically stable intermediate. Heating the reaction to ambient temperature induces reductive elimination and the oxidative addition into the carbon–bromine bond of the product. This newly formed nickel species can be cooled again to react with a deprotonated bromothiophene in the next cycle. Nevertheless, precise stoichiometric control of each step needs to be maintained to obtain high purity oligomers.

The iterative synthesis of discrete oligo dimethylsiloxanes (oDMS) has received significant attention in the field of macro-organic chemistry[57] and has recently been described by the Meijer group.[58,59] The general strategies toward both asymmetric (with a single endgroup for further functionalization) and symmetric (both endgroups functionalizable) are depicted in Figure 3. Formation of the oligosiloxanes was reliant on two key steps: (1) transformation of a siloxane hydride into the corresponding silanol and (2) subsequent condensation of the silanol with the chlorosilane building block **3**. In case of the asymmetric siloxanes, repetition of

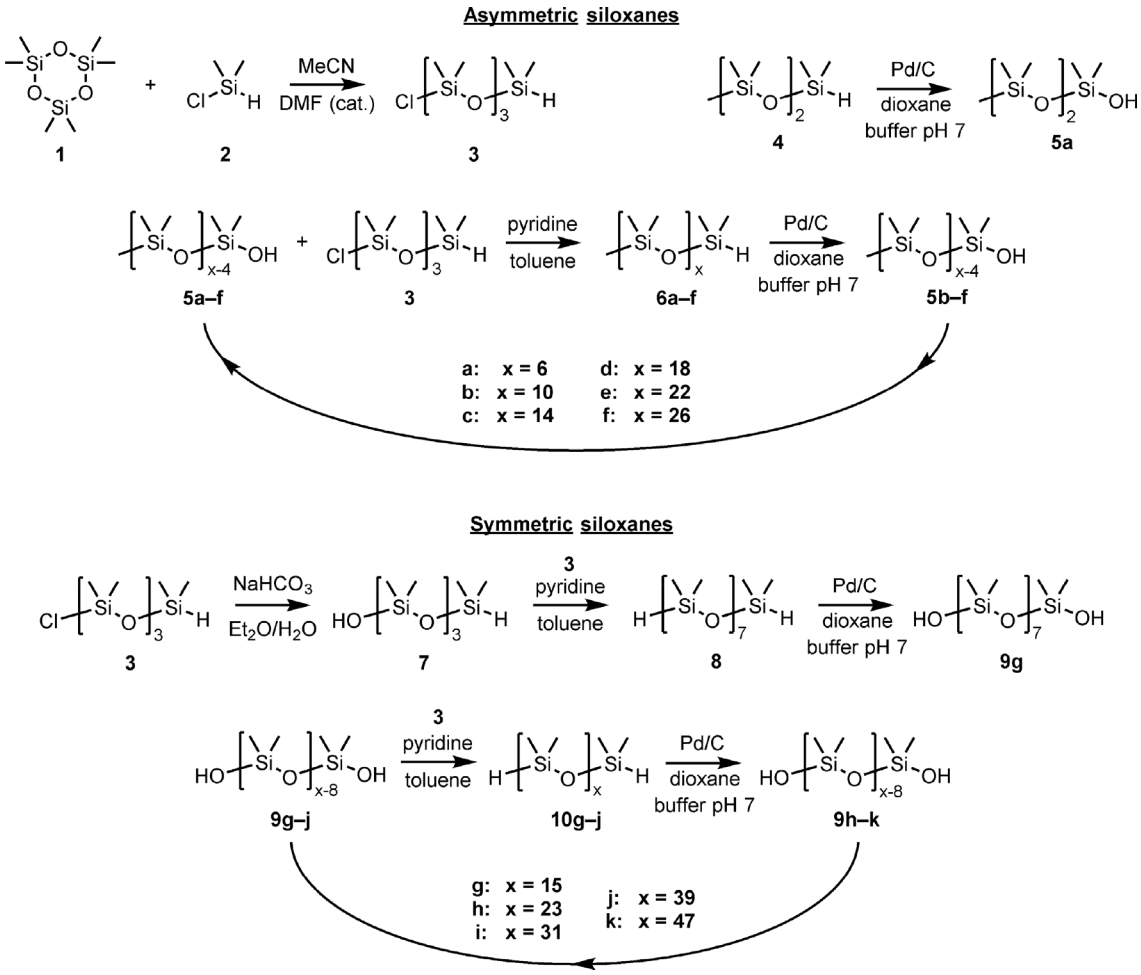

FIGURE 3 Synthetic routes toward asymmetric and symmetric oligodimethylsiloxanes. Adapted with permission.[58] Copyright 2016, American Chemical Society

these two steps adds four siloxane repeat units in each cycle. Thus, siloxanes with up to 27 repeat units were obtained starting from trisiloxane hydride **4**. Analogously, longer, symmetric siloxane oligomers were more conveniently prepared by employing a bidirectional growth strategy, starting from octasiloxane dihydride **10**.[60] The success of both routes greatly depends on the relative ease with which large quantities of bifunctional chlorosilane building block **3** could be produced and purified. The high purity of this material is crucial, as separation of higher MW siloxanes varying a few repeating units is practically impossible. It is particularly noteworthy that oDMS showed a large endgroup dependence (either hydride or silanol) on the adsorption to silica, regardless of the oligomer length. This allowed for the development of semi-automated purification protocols using standard column chromatography techniques to give excellent purity of the final products.

Matsumoto and coworkers presented a different approach toward oligo siloxanes based on $B(C_6F_5)_3$-catalyzed chemistry.[61] In the first step, dehydrogenative cross-coupling of alkoxysilanes with hydrosilanes was performed leading to a disiloxane with a Si–H terminal group. The terminus was next functionalized via hydrosilylation of a carbonyl compound to give an alkoxysilane capable of starting the cycle again. The iterative reaction could be performed in one pot, though the utilized carbonyl compounds had to be chosen carefully for efficient reaction. Sequence-controlled oligosiloxanes could be prepared via addition of different dihydrosilanes with the method being further extended to branched and cyclic siloxanes.

A strategy to tackle the considerable challenge of scalability in linear growth approaches is a transition to flow-based synthesis. For example, Xu and coworkers utilized photochemical activation of RAFT groups for single monomer unit insertions of *N*-phenyl maleimide and indene on a gram scale with the use of a flow setup.[62] In a similar way, Barner-Kowollik and coworkers employed photochemical activated Diels–Alder chemistry to synthesize sequence defined oligomers in flow.[63]

Recently, Percec and coworkers introduced the concept of self-interrupted living polymerization for the

synthesis of well-defined oligomers.[64] Therefore, a common chain growth polymerization method, that is, ring-opening metathesis polymerization, was utilized. In order to control the chain growth process with regard to the chain length, oxanorbornene monomers with bulky dendrimer substituents are introduced. During the propagation, the growing oligomer chains self-assemble into spherical structures that effectively block monomer addition at a DP of 16. Hence, discrete oligomers were obtained in a one pot reaction utilizing a chain growth process and supramolecular assembly without any additional separation or protecting group chemistry.

2.1.2 | Exponential growth

The iterative exponential growth strategy (IEG, also frequently named divergent/convergent approach) is presently the most efficient process for the scalable synthesis of discrete, high molecular weight oligomers (Figure 1). The key concept in this approach is the use of a bifunctional building block, of which both functionalities (*X* and *Y*) can react with each other, leading to coupling. To prevent uncontrolled coupling or polycondensation, the use of orthogonal protecting groups or orthogonal chemistries is required, allowing deprotection or activation of the two end groups separately (the divergent step). Subsequent ligation of these two mono-activated components (the convergent step) leads to materials that regain two, non-reactive end groups with an overall doubling of the number of repeating units. With this higher-molecular weight material, the divergent/convergent process can be repeated until the desired molecular weight is reached, and purification at each step is greatly facilitated by the dramatic increase in molecular weight at each step. While drawbacks of the exponential growth include reduced flexibility for inserting chemically different monomer residues and the need for orthogonal reactions to protect the end groups, it is a versatile approach for the synthesis of large periodic oligomers.

The accelerated formation of oligomers via exponential growth strategies has been widely used, starting with the development of large scale synthesis of discrete hydrocarbons for use as model systems for paraffin and polyolefins.[65–68] In a synthetic tour de force, Dixon and coworkers synthesized tetranonacontane ($C_{94}H_{190}$) on a 100 g scale[69] while Whiting prepared multiple libraries of linear and branched alkanes.[70–73] In these systems, a combination of Baeyer–Villiger reaction, acetal formation and Wittig reaction was utilized to grow hydrocarbon chains with internal alkenes in an exponential manner that could be converted to discrete hydrocarbons after hydrogenation. The systematic process developed by Whiting and coworkers allowed the fabrication of alkanes, up to nonacontatrictane ($C_{390}H_{782}$), as well as customized per-polydeuterated compounds[74] in high purity which were critical for understanding the fundamental crystallization behavior of commercially important polyolefin systems.

Polyesters embody a second family of commercially relevant materials that are ideal candidates for IEG strategies. A seminal example is the work of Seebach and coworkers,[75] where a route toward oligomers of (*R*)-3-hydroxybutyric acid from the dimer up to the 128-mer was developed (Figure 4). Their strategy employs two different protecting groups for the hydroxyl and carboxyl termini of the mono- and oligomers, a *tert*-butyldiphenylsilyl ether and a benzyl ester (**11**), respectively. Selective removal of these groups could be achieved either by Pd/C catalyzed hydrogenolysis or treatment with HF·pyridine complex to give chain end differentiated oligomers with either a free carboxylic acid (**12**) or alcohol (**13**) functionality, respectively. Transformation of the acid into the acid chloride and coupling with the corresponding hydroxy-terminated oligomer results in the chain extended product **14**, which effectively is the dimer of **11**. Repetition of this deprotection/coupling sequence gave oligomers with 2, 4, 8, 16, 32, 64, or 128 repeat units. As noted by the authors, the coupling and subsequent purification of the reaction mixture became increasingly difficult for longer oligomer lengths despite the dramatic increases in molecular weight. Later, Hawker and coworkers prepared 64-mers of ε-caprolactone and lactic acid with purities above 95% using differentially protected monomers following the Seebach strategy.[76,77]

Also noteworthy is the synthesis and full characterization of oligomers with up to 64 butylene glutarate residues by the group of Chapman, who employed 9-fluorenylmethoxycarbonyl (Fmoc) and benzyl ether protecting groups to enable IEG.[78] This success prompted the investigation of other condensation systems. An illustrative example is the straightforward solution-phase protocol toward nylon-6 mimics in the form of uniform 6-aminohexanoic acid 32-mers by Whiting and coworkers which used ethyl ester and *tert*-butoxy carbonyl groups for differential protection.[79,80] Very recently, Kim and coworkers presented the synthesis of sequence defined poly(phenyl lactic acid-*co*-lactic acid).[81] The oligomers were synthesized in a hybrid approach consisting of the synthesis of building blocks with 4 monomer units and further coupling to oligomers with lengths up to 64 units. In the last step the stored sequence information was extracted via matrix assisted laser desorption ionization time of flight mass spectrometry/mass spectrometry (MALDI-ToF MS/MS) experiments. In another work, the same group synthesized discrete poly(lactic acid) with DP

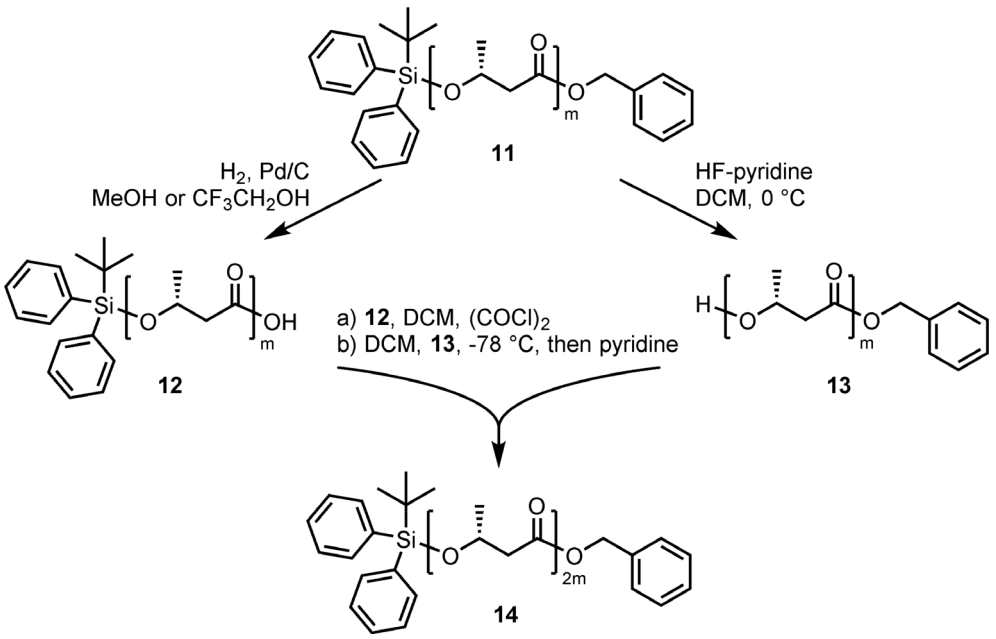

FIGURE 4 Iterative exponential growth (IEG) strategy for oligo((*R*)-3-hydroxybutyric acid) up to the 128-mer. Adapted with permission.[75] Copyright 1996, John Wiley and Sons

up to 1024.[82] Furthermore, cyclization was applied via CuAAc to obtain discrete cyclic poly(lactic acid) (DP up to 512) and poly(phenyl lactic acid)-*b*-poly(lactic acid) (DP up to 64 + 64).

The widespread use of poly(ethylene glycol) (PEG) in biological and biochemical contexts has similarly driven interest in the synthesis of discrete PEG oligomers of uniform length with the landmark 1939 paper of Fordyce and Hibbert illustrating the preparation of an oEG 42-mer.[83,84] Almost 70 years later, a longer oligomer, comprising 44 repeat units was synthesized by Tanaka,[85] and the preparation of multigram quantities of lower-molecular weight compounds was achieved by the group of Hill.[86] In 2009, Davis and coworkers successfully synthesized discrete PEG_{48} in greater than 98% purity using *tert*-butyl, benzyl and trityl protecting groups in combination with tosyl activation and chromatographic purification.[87]

A creative route to uniform (block) co-oligomers (BCOs) based on ethylene glycol repeat units and modifiable side-groups was reported by the group of Johnson.[88,89] In these studies, CuAAc is employed to prepare uniform oligomers consisting of two different monomer residues and up to 32 repeat units. The basic strategy is depicted in Figure 5 and shows the synthesis of azide and alkyne functionalized monomers **15-N_3** and **15-alkyne** from a common precursor. Also notable are the masked end groups where an alkyl bromide acts as a precursor for the azide and a triisopropylsilyl (TIPS) group protects the alkyne. Both monomers could be selectively coupled via CuAAC, resulting in the "inert" triazole dimer with protected end groups. Selective transformation to the azide with sodium azide and the free alkyne with tetrabutylammonium fluoride led to different intermediates, which was followed by coupling of the fragments with CuAAc to give the tetramer. Iteration of this process leads to higher-molecular weight compounds with uniform lengths, as evidenced by the high-resolution mass spectra (Figure 5). Of particular note is the presence of allyl groups on the backbone which allows secondary functionalization of the oligomers with thiol-ene chemistry,[88] in turn permitting the generation of BCOs with further sequence diversity. In a similar way, Fernandes and coworkers utilized CuAAc to synthesize discrete oligomers with control over chiral centers along the chain with inclusion of various functional groups along the chain, for example, alkyl, phenyl, pyridyl, hydroxyl, amine, imidazole, and carboxylic acid functions.[90] A combination of thiol–maleimide Michael coupling reactions and orthogonal chain end deprotections based on a retro-Diels–Alder approach were employed by Zhu to prepare discrete molecular weight materials up to the 128-mer with the reported purity of the longest oligomer being ~95%.[91] With both of these strategies, materials were developed that have no structural analog to traditional polymer classes or biopolymers, highlighting the opportunities in new chemical space that can be explored by the use of robust and orthogonal chemistries.

Remarkable advances have also been achieved in the synthesis of discrete-length conjugated polymers.[25] Efforts in this area were pioneered by the Tour group, where sequential halogenations and Sonogashira cross couplings led to the rapid construction of conjugated oligomers up to 16 units in length.[92] Although direct synthesis of oligomers with 20 or more repeat units is rarely performed, notable examples of oligomers with extreme

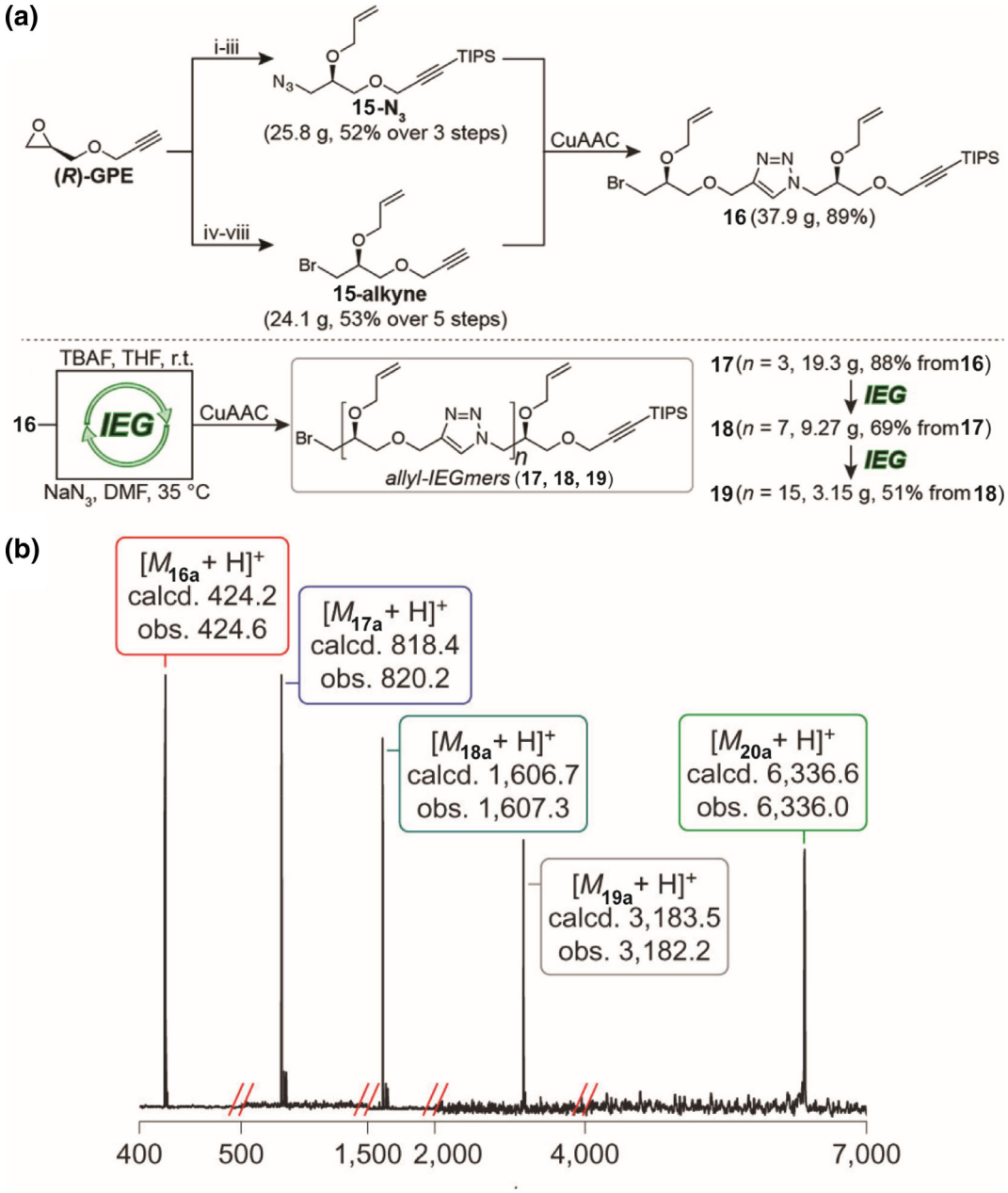

FIGURE 5 (a) Fabrication of uniform oligomers up to 16 repeat units with azide-alkyne click chemistry (adapted with permission.[65] Copyright 2016, American Chemical Society.) and (b) high-resolution MS data for a number of the discrete-molecular weight materials. (reprinted by permission.[66] Copyright 2015, Springer Nature

lengths were reported from the group of Osuka.[93,94] For example, linear polyporphyrins with up to 1024 repeat units ($C_{65536}H_{83970}N_{4096}O_{4096}Zn_{1024}$) were prepared by iterative homodimerization and recycling size exclusion chromatography (SEC) purification steps.[93] These ultra-high molecular weights illustrate an underlying challenge of accurate characterization with discrete large oligomers/polymers, as mass spectrometric confirmation of the products was only possible up to the 128-mer. Heeney and coworkers displayed a more systematic strategy for obtaining regioregular oligothiophenes that was less reliant on state-of-the-art recycling SEC equipment.[95,96] Based on selective bromination and stannylation reactions at the 2 and 5′-positions of the oligothiophene termini, desymmetrized building blocks were coupled by means of a Stille reaction. By following the Fibonacci sequence when selecting two monofunctional blocks for ligation, purification was facilitated and lengths up to the 36-mer became available (Figure 6). In addition to these discrete oligomers, high-molecular weight conjugated

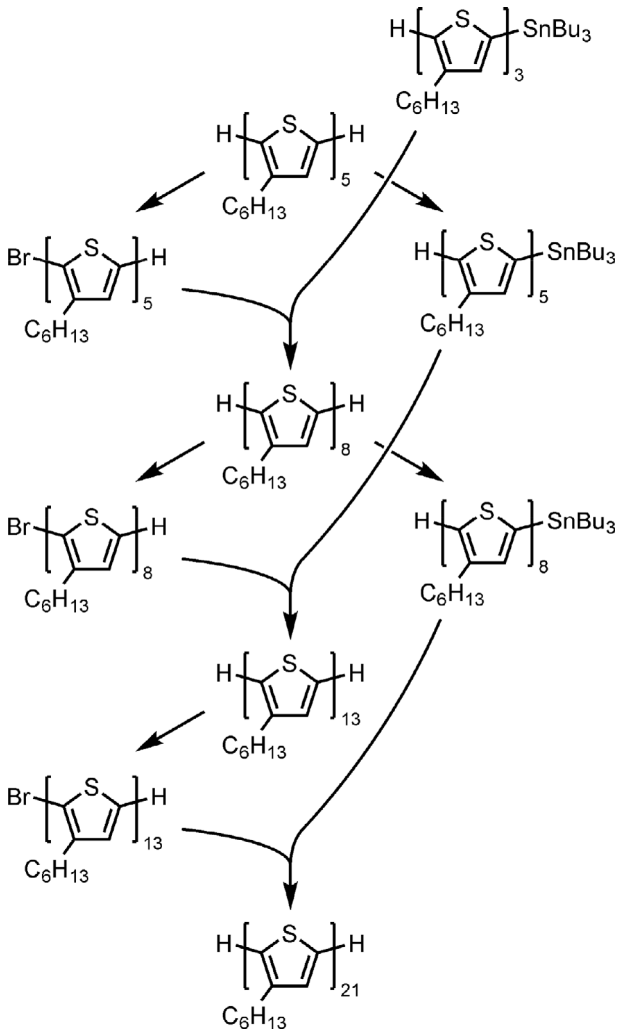

FIGURE 6 Iterative exponential growth toward oligo thiophenes via a combination of selective bromination and Stille coupling. Adapted with permission.[95,96] Copyright 2013, American Chemical Society 2013

polymers can also be obtained by the ligation of pre-made oligomeric blocks, as illustrated by the work of Otsubo.[97] The progress in the field can be illustrated by the synthesis of substituted 2,2′:5′,2″:5″,2‴:5‴,2⁗:5⁗,2⁗′:5⁗′,2⁗″:5⁗″,2⁗‴:5⁗‴,2⁗⁗:5⁗⁗-undecithiophenes.[98] Published in 1991 as the longest characterized oligothiophene, strategies for the preparation of higher oligomers followed quickly thereafter.[92] Wang et al. synthesized discrete poly(fluorene) via an iterative Suzuki coupling approach to yield discrete oligomers up to a DP of 64.[99]

2.2 | Defined oligomers via purification

As outlined above, stepwise synthetic methods have been very successful in producing oligomeric materials of precise length from a wide variety of building blocks. However, the multi-step nature is inefficient for preparing large libraries of discrete oligomers and can be challenging for non-experts. To address these challenges, separation-based strategies have been developed to isolate individual oligomers from disperse materials. In these systems, libraries of material are formed from a single synthetic step to give oligomers that are frequently inaccessible through iterative synthesis methods (Figure 7). Current limitations of this method are reduced separation with higher molecular weight oligomers and decreased statistical yield of any one oligomer length at higher DP. The genesis of these strategies can be traced back to the analytical analysis of oligomer mixtures using affinity-based chromatography techniques. For example, Chang and coworkers have shown that low dispersity polystyrene-*b*-polyisoprene (PS-*b*-PI)[100,101] and polystyrene-*b*-poly(methyl methacrylate) (PS-*b*-PMMA)[102] with relatively high average molecular weight (20–80 kDa) can be fractionated into samples with dramatically reduced molecular dispersities ($Đ < 1.01$) utilizing preparative high-performance liquid chromatography (HPLC). At lower molecular weights (2.4 kDa), separation into discrete-length oligomers could be achieved leading to unique block structures. While only available at an analytical scale, these systems do pose an interesting and open question regarding the relative dispersity of individual block lengths and if chromatographic separation can separate overall molecular weights as well as individual block lengths.[101]

These initial studies were then followed by a series of reports illustrating the preparation of uniform oligomers by fractionation of low molecular weight, disperse mixtures. For example, milligram quantities of oligo(pyrrole-2,5-diyl)s up to the 20-mer with purities >90% have been obtained by preparative HPLC of a disperse mixture,[103] while the chromatographic separation of ethylene oxide oligomers allows for the isolation of 32- and 48-mer oligo (ethylene glycol) derivatives.[87] In all cases, the primary drawback of these approaches is the limited scalability.

With the advances in automated chromatography systems, these challenges could be addressed using the preparative scale isolation of discrete-length oligomers of oligoacrylates, oligostyrenics, and oDMS. With the automated flash chromatography approach,[104] these protocols were extended to conjugated oligomers and oligovinylacetates with a major advantage being the ability to start from commercially available materials (Figure 8).[105,106] This allows large scale separations (2 to >10 grams) to be conducted leading to practical quantities of individual oligomers with lengths up to approximately 15 repeat units. In addition to the significant decrease in synthetic complexity, this approach is also applicable to libraries of oligomers, such as vinyl-based addition

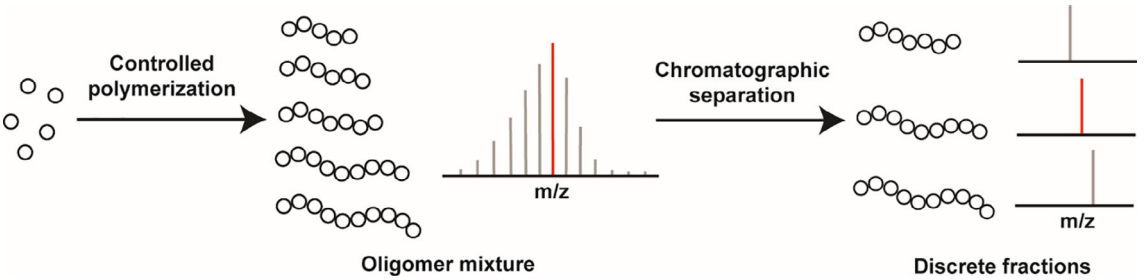

FIGURE 7 Schematic overview for the synthesis of discrete oligomers via chromatographic separation

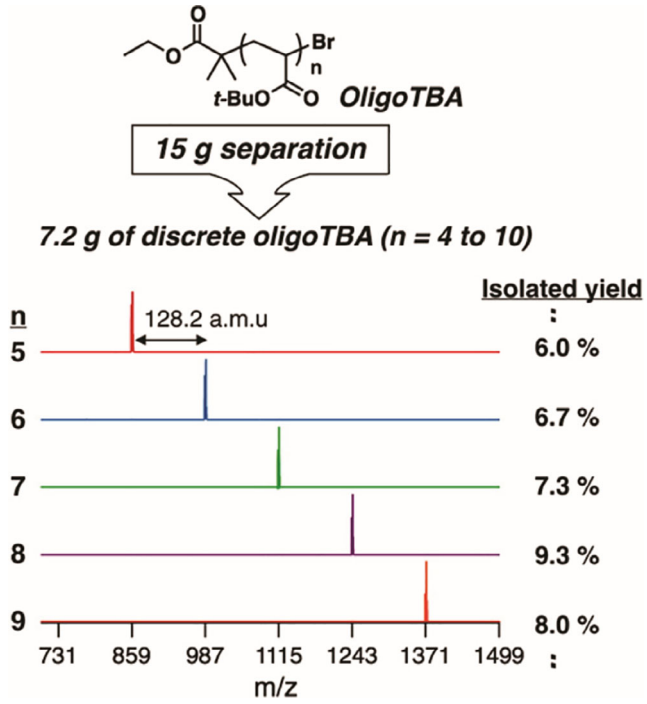

FIGURE 8 MALDI-TOF MS spectra of discrete-length oligo (*tert*-butyl acrylate) with 5–9 repeat units isolated on gram scale after chromatographic separation of a disperse mixture. Reprinted with permission.[104] Copyright 2016, American Chemical Society

polymers, that are traditionally challenging to prepare in a stepwise manner (vide infra). Hoshino and coworkers utilized affinity chromatography to purify oligomers that were designed to interact with short peptides.[107] The oligomers were formed from *N*-isopropylacrylamide (NIPAM) and *tert*-butyl acrylamide via RAFT polymerization. The target peptides could be immobilized on beads and loaded into a chromatography column with the synthetized oligomers separated according to their interactions with the respective peptides (refer to Section 3.3.2).[108]

Hybrid methodologies that combine stepwise strategies with purification of oligomer mixtures have recently been developed and offer gains when compared to traditional approaches, especially to higher molecular weight systems. This is exemplified by the synthesis of well-defined conjugated materials by Otsubo and coworkers.[97] By initially preparing uniform octa(thiophenes) with acetylene end groups, subsequent oxidative coupling leads to a mixture of oligo(octathienylene–diethynylene)s with the oligomerization reaction being modulated by the molar ratio of monofunctional units which serve as end capping agents. As the "monomer" is an oligomer itself, the considerable molecular weight differences between coupled products facilitates separation by preparative SEC. From this library of 8-mers, multiple discrete high molecular weight oligomers, up to 13.8 kDa consisting of 96 thiophene repeat units, could be obtained.

In a related study, an iterative protocol based on reversible deactivation of radicals has been developed by Junkers and coworkers (Figure 9).[109] Using copper-catalyzed photoinduced radical addition chemistry, single additions of acrylates to α-bromo esters leads to statistical radical insertion, with chromatographic methods being utilized to obtain discrete materials after each insertion step. The generality of this strategy was further illustrated by using RAFT procedures for single monomer insertions to give oligomer libraries[110] with automated column purification resulting in sequence controlled oligomers.[111]

These strategies could also be used for the rapid generation of block copolymer libraries spanning a wide range of compositions starting from a single parent copolymer.[112] This versatile and scalable strategy employs automated and operationally simple chromatographic separation that is demonstrated to be applicable to a variety of block copolymer chemistries on multigram scales with excellent mass recovery. To illustrate the utility of this approach, poly(dodecyl acrylate)-*block*-poly(lactide) (PDDA-*b*-PLA) was used as a model and automated fractionation of this PDDA-*b*-PLA sample (2.5 g) was completed within 1 h using a commercially available silica

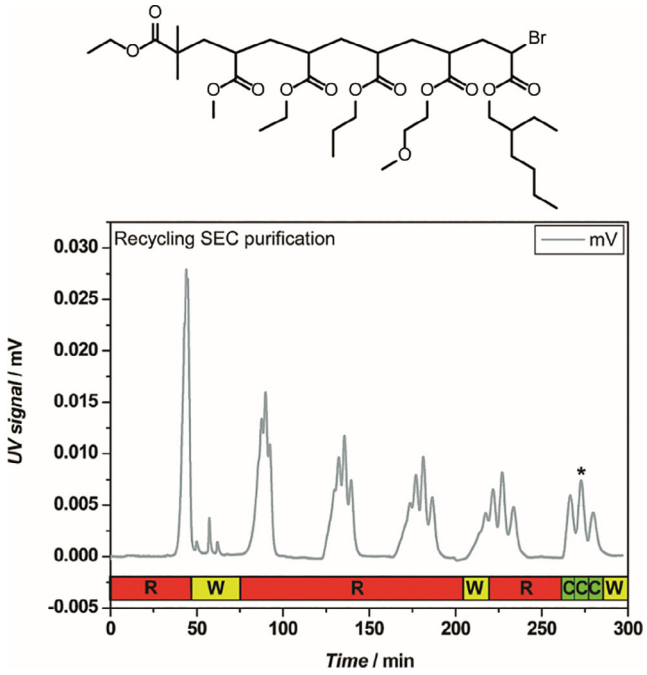

FIGURE 9 Recycling SEC trace recorded during consecutive purification cycles of an oligo(acrylate), (letters R, W, and C standing for recycle, waste and collect; the desired oligomer is marked with an asterisk). Adapted from Reference 109, licensed under CC-BY

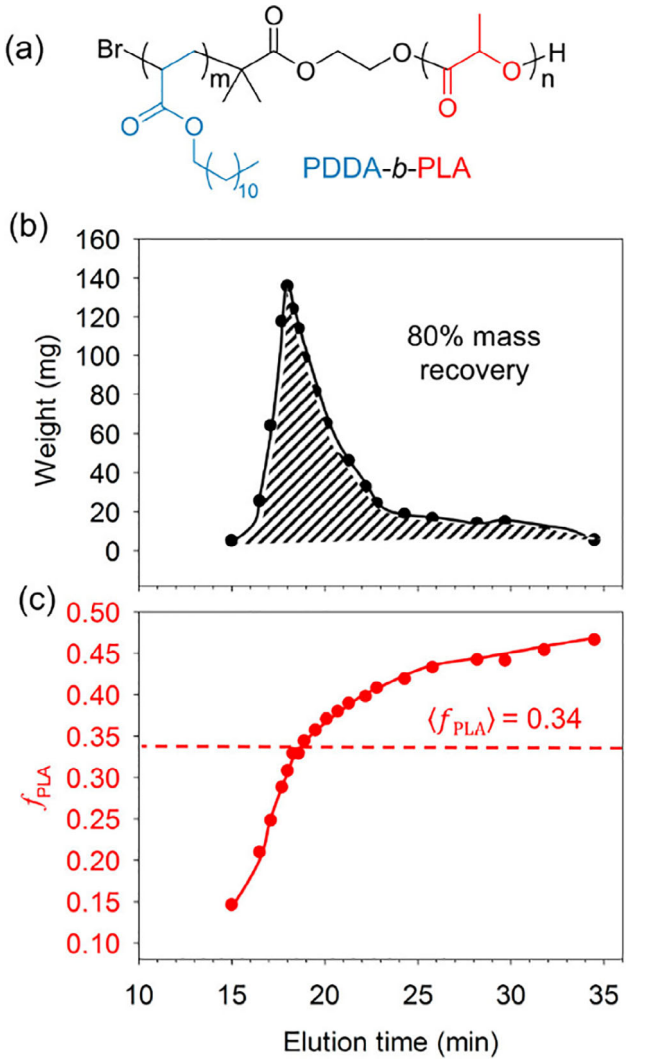

FIGURE 10 (a) Molecular structure of PDDA-*b*-PLA, chromatographic separation of a single BCP parent material (2.5 g, $\langle M_n \rangle$ = 4000 g/mol) produces a series of fractionated samples obtained with increasing elution time: The isolated mass (b) and composition of each fraction (c). The dashed red line represents the average composition of the starting, parent PDDA-*b*-PLA. Reprinted with permission.[112] Copyright 2020, American Chemical Society

chromatography column and an evaporative light-scattering detector. Figure 10 illustrates the successful fractionation of the starting PDDA-*b*-PLA copolymer into 20 well-defined BCP samples (10–100 mg each) with an overall mass recovery of 80%.[112]

As exemplified by the examples above, discrete oligomer synthesis requires both high yielding transformations and preferably, efficient methods to purify the intermediate and final compounds. Depending on the desired molecular weight and structural complexity, a variety of strategies are available, each having advantages depending on the nature of the oligomer. If uniform materials based on a single type of monomer unit, are required, exponential growth strategies provide an efficient and scalable approach. For sequence defined oligomers, stepwise and potentially automated strategies allow for control over monomer sequence leading to unprecedented understanding of structure–property relationships for a wide range of polymer families. In all areas, the examination of libraries of discrete oligomers leads to a fundamental comprehension of the ensemble properties and morphologies of the corresponding polymeric systems. The opportunities for future study at the interface of oligomer chemistry and polymer physics will be highlighted in the next section.

3 | PROPERTIES OF OLIGOMER-BASED MATERIALS

The prospect of controlling macroscopic properties through the addition of a single monomer unit or inversion of a stereocenter is a driving force for oligomeric materials research. These effects can take many forms, ranging from bulk thermal properties to solution self-assembly to catalysis. While the oligomer synthesis can be time-consuming, the resulting precision offers unparalleled opportunities to tailor a material toward a given application and leads to fundamental understanding that

could not be gained through other means. For example, the combination of crystallinity and self-assembly in discrete block co-oligomer systems gives rise to a blurring of boundaries between the fields of oligomer chemistry and liquid crystalline (LC) assembly. The work of Moore and coworkers with regard to foldamers[113] clearly illustrates the promise of systematic varying oligomer DP followed by molecular-level characterization for defining structure property relationships. In the following section, additional examples will highlight this paradigm and define opportunities for future applications.

3.1 | Oligomers in the bulk

3.1.1 | Thermal properties

One of the most explored areas of macro-organic chemistry is the modulation of thermal properties, such as glass transition temperature (T_g), melting temperature (T_m), or crystallization temperature (T_c). It has long been appreciated that the T_g of a disperse material increases as it transitions from an oligomer to polymer, and recent synthetic advances permit this effect to be evaluated for defined oligomer systems with increased resolution and with regard to sequence. This leads to the tuning of these thermal parameters in a broad window of temperatures, which directly impacts the processability of oligomeric materials. For example, in the areas of additive manufacturing or injection molding which target applications such as biomedical implants or organic electronics.

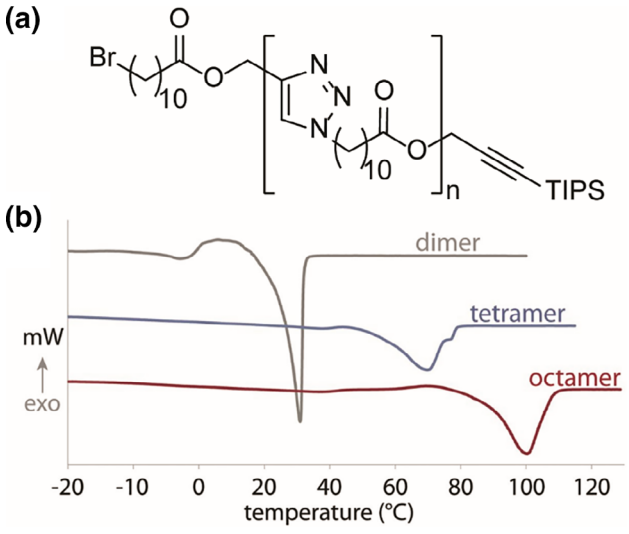

FIGURE 11 (a) Molecular structure of aliphatic oligo ester and (b) dynamic scanning calorimetry traces obtained from an aliphatic oligo ester showing the increase in T_m with number of repeating units. Reprinted from Reference 114, licensed under CC-BY

An excellent example of modulating thermal properties through oligomer design is demonstrated by Leibfarth, Johnson, and Jamison where a library of aliphatic oligo esters from dimer to octamer is studied (Figure 11).[114] These oligomers were produced using an IEG strategy (Section 2.1.2), with the process greatly streamlined by performing the synthesis in flow, termed Flow-IEG. Glass transition temperatures were found to increase from −53.1°C for the dimer to −23.9°C for the tetramer, and further to −16.5°C for the octamer. The melting points of the same oligomers spanned a ∼70°C range, with a T_m of 31.0°C measured for the dimer and increasing to 100.4°C for the octamer. The corresponding polymer had a T_m of 112°C indicating the low DP for attaining the ultimate oligomer-to-polymer property transition. The authors also highlighted the importance of oligomer sequence on these properties, which is readily achieved by using either aliphatic or diethyleneglycol derived monomers in the coupling steps. When a 16-mer containing alternating sequences $(ABAB)_n$ was prepared, it displayed a T_m of 44°C. In contrast, the double alternating sequence $(AABB)_n$ isomer had two melting points, at 29 and 64°C respectively, The same group further demonstrated that the triazole substitution pattern (1,4 vs. 1,5) altered the thermal properties, in addition to length and sequence.[115] While the specific origins of these differences are not fully understood, this further reinforces the subtleties of macro-organic materials and the potential to control materials properties through small structural changes. These studies also represent a major opportunity to generate custom materials that feature specific thermal transitions or combinations of thermal properties through the use of block polymers.

3.1.2 | Crystallinity

Crystallinity has been heavily studied in both polymer science and small molecule research. As long-range order is a necessity for any crystallization process, discrete oligomers present a rational framework to study the structural requirements for efficient crystallization. Major effects on crystal structures were reported, implying the potential of crystalline oligomer materials and the associated implications for applications and tailoring of material properties via oligomer design.

One of the most important semicrystalline polymer materials is PEG due to its widespread use in the biomedical field. In order to study the crystallization behavior of oEG, Davis and coworkers synthesized oEG through an IEG approach and studied the impact of oligomer

length.[87] After probing this system via single crystal XRD, a 3_{10}-helix was found, which is similar to the α-3_{10}-helices found in natural polypeptides. The results show that discrete oligomer structures can have a significant effect on single crystal formation as similar ordered structures could not be observed in disperse oEG.

Another material class that relies strongly on crystallization for performance is conjugated polymers, which are frequently utilized for optoelectronic devices. In the realm of conjugated oligomers, Smith and coworkers studied the thermal and crystallization behavior of o3HT with the number of repeating units ranging from a 4-mer to the 36-mer.[95] Two crystal morphologies were observed that were dependent on the number of repeating units. Form I is typically observed for higher molecular weights (above 21 repeating units). It features a high nucleation rate, and is kinetically favored. Form II is observed for lower molecular weight oligomers (below 9 repeating units) and is characterized by high order in the solid-state with sidechain interdigitation leading to lower rates of nucleation. For intermediate DP's, both crystal morphologies can be present depending on thermal treatment and the crystal morphologies can be converted reversibly. Later, Hawker and Kim et al. confirmed the appearance of two crystal structures depending on the molecular weight of the o3HT.[116] Moreover, they showed that the thin film crystal orientation of the oligomers changes from edge-on to face-on as the DP decreased below 12. For the field of conjugated organic electronics, parameters such as DP and dispersity are of vital importance with control over the morphology having direct impact on potential applications.

Interestingly, the previously described chromatographic separation of oligomers by Hawker and coworkers also allows TBA oligomers to be separated according to their stereochemistry as well as DP.[104] For a series of pentamers, different physical properties were observed that ranged from a waxy to a semicrystalline solid. Further analysis of each of these samples by NMR demonstrated distinct tacticities associated with each fraction. The isolation of both waxy and semicrystalline fractions was also possible for higher molecular weight hexamer and heptamers, leading to even greater diversity of materials. Additional examples of stereochemistry impacting properties and crystallization behavior can be found for isotactic lactic acid oligomers, synthesized from enantiopure starting materials using the IEG strategy developed by Seebach.[75] Hawker and coworkers first showed the effect of repeating units on the crystalline packing of oligo-L-lactic acid derivatives (oLLA).[77] Lamellar structures with a thickness matching the oligomer length were observed, with the only exception being the 64-mer having a lamellar thickness that is half of the extended molecular length. This indicates chain folding for the 64-mer, which was also found by Meijer and coworkers who extended the studies on oLLA crystallization.[117] Discrete length oLA stereocomplexes were formed upon mixing oLLA with the enantiomeric oligo-D-lactic acid (oDLA) of equal length. Herein, folding of the 64-mer was unfavorable due to a tighter packing of the stereocomplex into a 3_1-helix instead of a 10_3-helix for the homochiral oligomers. These studies clearly show the close relationship between molecular structure – both length and tacticity – with crystallinity and the resulting mesoscale organization.

The effect of oligomer length on crystallinity was also shown for oligo(ε-caprolactone) (oCL) by Hawker and coworkers (Figure 12).[76] A series of oCL oligomers (octamer to 64-mer) displayed a lamellar morphology by SAXS, with the domain spacing correlating to the theoretical length of a stretched oligomer unit for the octamer and 16-mer samples. In contrast, for the 32-mer, lamellae thicknesses were observed significantly below the calculated length of the oCL molecules (∼50%) indicating folding of the oligomer chain. The 64-mer displayed a thickness ∼30% of the calculated length, corresponding to multiple folds of the oligomer chain. AFM was also employed to probe the crystalline domains of 32-mer and 64-mer caprolactone oligomers and well-defined crystalline domains with sizes of 30 and >100 μm were obtained, respectively. This is in contrast to a commercial, disperse polycaprolactone (PCL) sample that led to a multitude of crystallites with sizes in the range of 10 μm. This example clearly shows the potential of defined oligomers to control structure on nanometer length scales. Although it may seem intuitive that different numbers of repeating units lead to different domain spacing, a high degree of crystallinity depends strongly on the uniformity of the oligomers with regard to their length.

In a similar way, the impact of oligomer length on thermal and crystalline properties of oligomers was studied for thiol-maleimide oligomers with hexyl spacers,[91] oligo(methyl methacrylate),[118] oligo(δ-valerolactone)[119] or oligo(di(ethylene glycol) ethyl ether acrylate)[118] materials. Not only were T_g and T_m significantly affected by the number of repeating units, but the thermal degradation temperature measured via TGA also depends on the oligomer structure as shown for oCL[76] and oLLA.[77] Overall, oligomer design and synthesis precision has a profound influence on thermal properties and crystallization that is a key feature for potential applications and associated processing windows. An area that still needs more examination is the impact of chain ends, which for low molecular weight oligomers may have an appreciable influence on polymer properties with Click strategies offering easy access to precision oligomer libraries.[120]

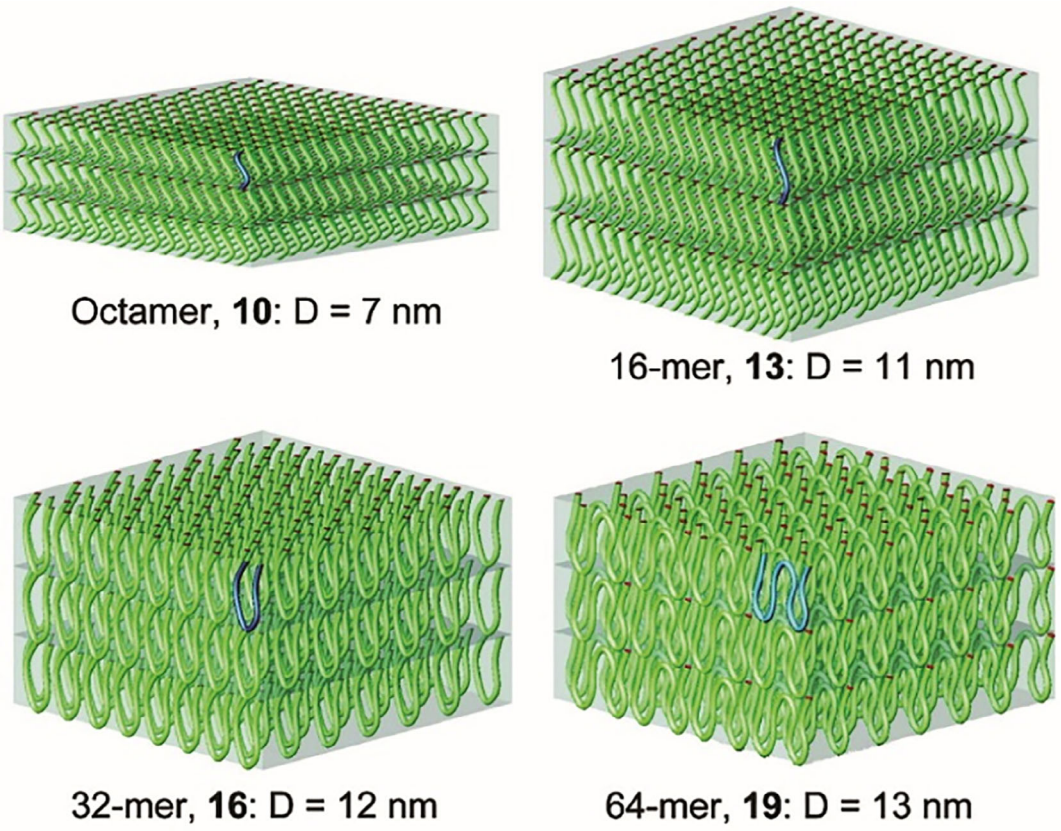

FIGURE 12 Structure of lamellar oligo(ε-caprolactone) (oCL) crystals with varied DP. Reprinted with permission.[76] Copyright 2008, American Chemical Society

3.2 | Self-assembly of block co-oligomers

3.2.1 | Phase segregation

Self-assembly of block polymers in the bulk and thin films via microphase segregation is a major driver for various applications. For example, in block copolymer lithography, smaller and smaller feature sizes are required for increased performance. In extending these studies to block co-oligomers (BCOs), microphase segregation strongly depends on DP and volume fraction with small feature sizes, that is, sub-5 nm, correlating to the low DP of oligomers. Commonly, BCOs with high interaction parameters (χ) are utilized to facilitate self-assembly at these low number of repeating units (N) and for monodisperse oligomers, the product (χN) is proposed to be greater than 10.5 for phase segregation to occur.[121,122] For thin film assembly, the choice of blocks is therefore limited to the strong segregation regime and to a select range of oligomer pairs.

Oligomers of oDMS have found wide promise in self-assembly processes due to high-χ values when combined with a range of different monomers. Disperse oDMS oligomers with monocarboxydecyl chain ends were studied by Alegría and coworkers with interesting self-assembled structures observed by SAXS and WAXS characterization.[123] This system showed the formation of two well-ordered phases with sub-10 nm domain spacing that were dependent on temperature. At temperatures below 230 K the supramolecular self-assembly of carboxylic acid dimers via H-bonding prevailed, while self-assembly of the alkane units into hexagonally packed cylinders occurred below 205 K. The utilization of discrete oDMS structures by Meijer and coworkers has highlighted the importance of dispersity with investigations on the formation of ordered structures via incorporation of an oLA block.[58] The discrete design allows for precise control over the block lengths resulting in the formation of lamellar, cylindrical and gyroid morphologies with similar self-assembled structures occurring in thin films of oDMS-*b*-oLA (Figure 13). AFM studies revealed minor height fluctuations from different numbers of polymer layers and a constant height difference of approximately 8.5 nm in the case of $oDMS_{27}$-*b*-oLA_{15}, which is in-line with the obtained bulk material SAXS results. In the case of $oDMS_{59}$-*b*-oLA_{33} a larger phase difference was

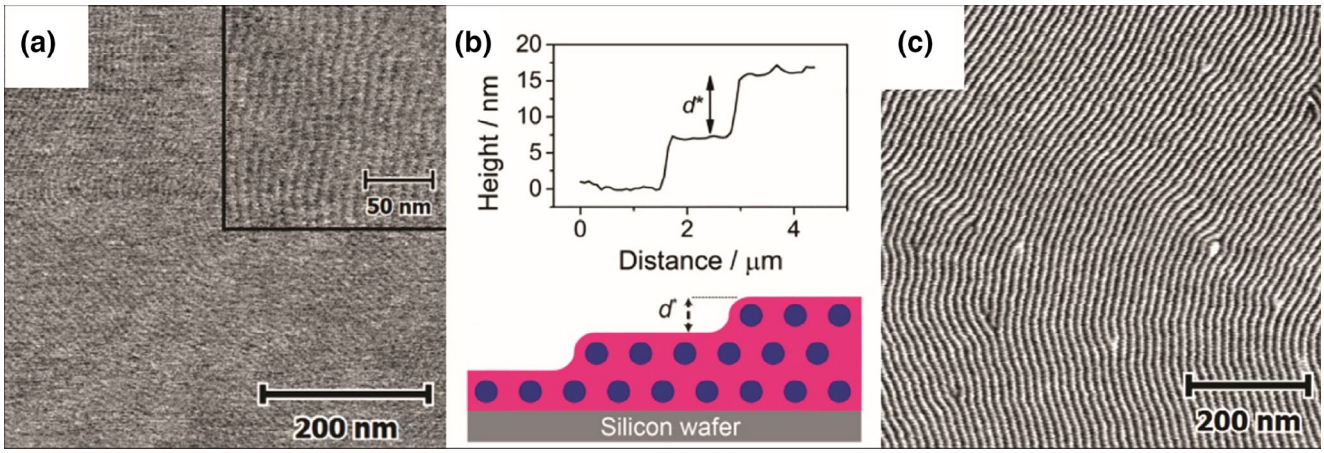

FIGURE 13 (a) Tapping mode AFM phase image of oDMS$_{27}$-*b*-oLA$_{15}$, (b) extracted height profile of oDMS$_{27}$-*b*-oLA$_{15}$, and (c) tapping mode AFM phase image of oDMS$_{59}$-*b*-oLA$_{33}$. Reprinted with permission.[58] Copyright 2016, American Chemical Society

observed due to stronger segregation. However, decreased long-range ordering was obtained at higher molecular weights due to lower chain mobility.

A more in-depth study of the oDMS-*b*-oLA system showed that switching from a discrete oligomer to a disperse BCO has two primary effects. The stability of the microphase-segregated state increased, while the overall degree of ordering decreased. The effect of increased segregation stability can be explained by enhanced interactions between the disperse oligomer blocks that possess increased oligomer lengths, while the effect of decreased ordering is due to a hampered packing of disperse blocks. In a related study, Hawker and coworkers studied the phase segregation of oDMS-*b*-oMMA.[124] Discrete, semi-discrete and disperse blocks were synthesized via CuAAc of oligomer precursors with varying purity. Consistent with results by Meijer, discrete oligomers showed a significant decrease in domain spacing and sharper scattering peaks by SAXS compared to the corresponding disperse structures. Moreover, the order–disorder temperature decreases with increasing dispersity, which points to a destabilization of the ordered phase. These studies highlight the power of BCOs in self-assembly with unprecedented ordering of morphologies and extremely small feature sizes being observed. This was further showcased by Dong and coworkers who obtained different complex spherical phases based on the change in a single repeat units for a series of precise oligomers.[125] Discrete length oDMS-*b*-oLA BCOs could also be synthesized with diverse architectures and compositions yielding various branched BCOs and stable, low-symmetry spherical phases.

As described above, stereochemistry can play a central role in the assembly of oligomeric materials. Johnson and coworkers studied the effect of stereochemistry on BCO self-assembly of discrete oligomers with pendant

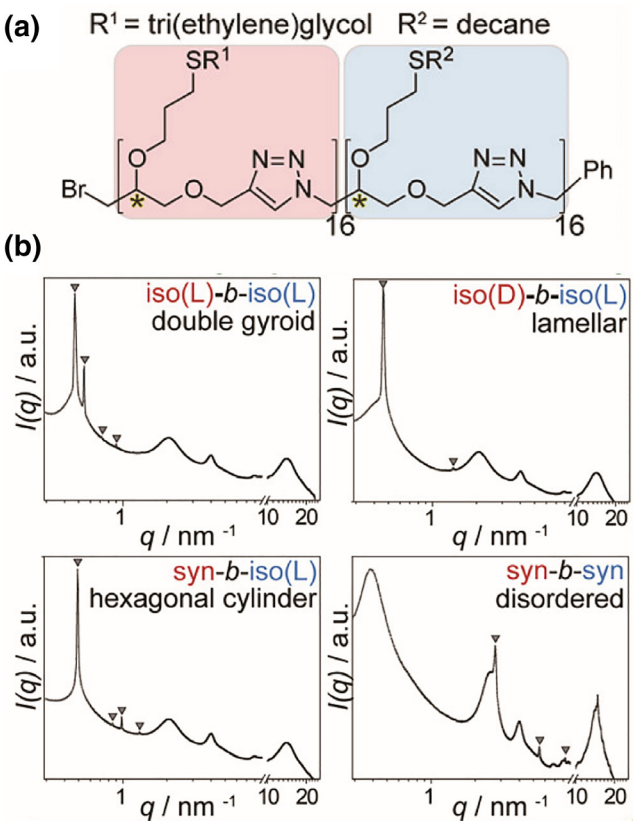

FIGURE 14 (a) Molecular structure of stereocontrolled CuAAc-derived oligomers and (b) SAXS data of stereocontrolled CuAAc-derived oligomers. Reprinted with permission.[126] Copyright 2018, American Chemical Society

allyl functionalities (Figure 14).[126] The stereochemical information was introduced through commercially available (*D*)- or (*L*)-epichlorohydrin building blocks and the allyl functions functionalized with tetra EG or decane

groups to obtain an amphiphilic BCO. Five combinations of blocks with different configurations and philicities were then assembled and segregation of each BCO was interrogated in the bulk via SAXS after thermal annealing. Interestingly, double gyroid, lamellar and hexagonal phases were observed depending on the stereochemistry of the blocks. The switch of one homochiral block from *L* to *D* resulted in a change from gyroid to lamellar morphology. Such a change in morphology was attributed to slight variations in the packing of the BCOs in space due to the orientation of the individual blocks. Changing the homochiral block in a different system to one with alternating *L*/*D* stereocenters led to further insights with the homochiral BCOs leading to well-defined self-assembled structures, while no ordering was observed for the alternating structure.

As solid-phase synthesis of oligomers has been greatly streamlined for biochemical and biomedical applications, chemists have also utilized these techniques for the fundamental studies of materials properties in the bulk for abiotic materials. Peptoids are analogs of traditional peptides that feature a shift of the sidechain from the α-position to the backbone nitrogen and have proved to be an important platform for studying self-assembly. For example, *N*-substituted glycine oligomers lack hydrogen bonding found in most traditional polypeptides and chirality of the backbone. This results in materials that are soluble in common organic solvents and behave as flexible chains. Using the submonomer approach, Balsara and Zuckermann synthesized a series of BCO peptoids in which one block contains a hydrophobic 2-ethylhexyl (Neh) sidechain and the other a hydrophilic triethylene glycol (Nte) sidechain (Figure 15).[127] The volume fraction of the Nte block was systematically varied from 0.11 to 0.65, while maintaining the overall chain length constant at exactly 36 units. When the volume fraction of Nte was 0.49 or less, these BCOs displayed lamellar phase separation with domain sizes between 7.1 and 6.2 nm. In further studies, these phase-separated materials were explored for application in lithium-ion batteries[128] and later extended to phosphonate containing BCOs for proton transfer membranes.[129] The results differ from classical block copolymer theory and therefore raise questions on the role of molecular architecture and molecular dispersity on the phase behavior of the diblock co-oligomers remain unknown.

Peptoids have also been used to examine fundamental questions in polymer science, such as the impact of chain stiffness on self-assembly. Using a diblock platform composed of disperse poly(*n*-butyl acrylate) (pBA) and discrete peptoid oligomers, Segalman and Zuckermann were able to tune the rigidity of the peptoid block through control of the secondary structure.[130] Utilization of a homochiral or racemic α-methyl benzyl side chain in the peptoid block generated sequences with either a stiff helical structure or

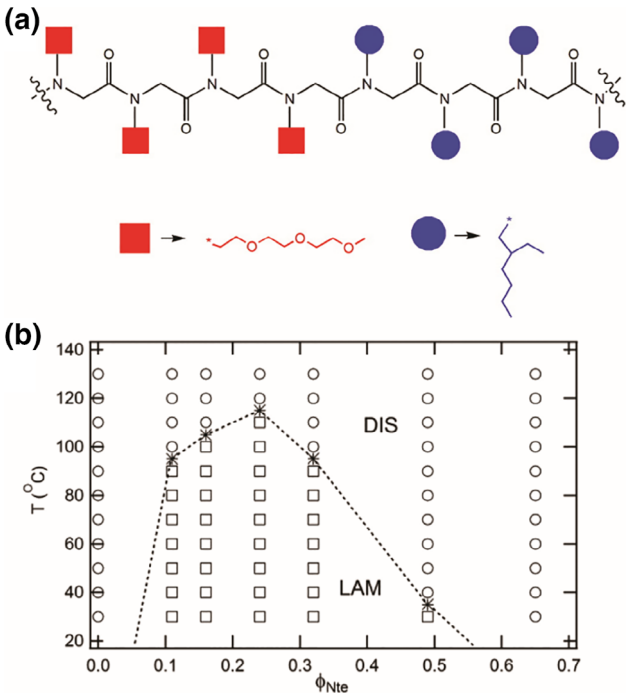

FIGURE 15 (a) Structure of the EG and ethyl hexyl-based peptoid BCO and (b) phase diagram for a peptoid BCO that demonstrates lamellar phase separation. Reprinted with permission.[127] Copyright 2013, American Chemical Society

an unstructured chain, respectively, with both types of diblocks self-assembling into hexagonal cylinders. Despite the helical block filling less space than the unstructured analog, larger domain spacings were observed for the chiral diblocks. Interestingly, for lamellae forming pBA-*b*-polypeptoid polymers, a domain spacing independent of the presence of secondary interactions was observed.[131] Herein, the impact of chain helicity on the thermodynamics of block copolymer self-assembly was studied yielding insight into the enthalpic and entropic contributions that arise from polymer chains with nonideal shapes in block copolymer self-assembly.

The limits of self-assembly governed by phase segregation were further pushed by Sita and coworkers using oligo(saccharide-olefin) conjugates.[132] Although, disperse olefins were utilized, remarkable nanostructures were obtained with the second "block" being a small molecule derivative. In an initial study, monosaccharides were coupled to oligo(propylene) or oligo(*iso*-butylene) derivatives via CuAAc. Both acetyl-protected and deprotected saccharides were studied as thin films via AFM showing segregated structures with feature sizes below 10 nm. In a similar way, a disaccharide-oligo(propylene) conjugate[133] revealed feature sizes of around 7 nm by GISAXS. Considering the length scale and design of these conjugates, which lies between small molecule surfactants and

amphiphilic block copolymers, correct nomenclature for this new class of macromolecules is open for debate. The future potential of these systems builds on the tailoring of the nanostructure via thermal annealing with changes in the morphology at physiological relevant temperatures driving applications in the biomedical field.

3.2.2 | Self-assembly driven by (liquid) crystallinity

The self-assembly of LC structures has been extensively studied due to their widespread applications in daily life such as liquid crystal displays and sensors. Phase segregated liquid crystalline structures have great potential for sub-5 nm patterning as additional interactions drive the assembly next to phase segregation. Domain sizes can be reduced due to the low molecular weight of the LC molecules and phase boundaries between the blocks are often sharpened due to a higher effective χ-parameter.[134] Structures that assemble through phase segregation in combination with (liquid) crystalline interactions have been broadly explored, including peptide rod-coil BCOs, amorphous-crystalline (discrete) BCOs, phase-segregated liquid crystals and block molecules. The latter term, block molecules, first introduced by Tschierske,[135] includes all macromolecules forming mesomorphic phases by phase segregation in combination with directional, crystalline interactions. Furthermore, crystallinity in all these types of oligomers can be a competing factor in the self-assembly process.[136] It should be noted that minimal connections between these fields is found in the literature.

Synthetic polypeptide-based block co-oligomers typically exhibit the phase behavior of rod-coil block copolymers due to the tendency of the rigid rods to form anisotropic domains. The domains originate from the formation of either β-sheets or the more common α-helices, as was shown by Lecommandoux and Klok through the study of low-molecular weight diblock co-oligomers consisting of styrene and benzyl glutamate.[137] Variations in block length ratio resulted in changes in the peptide structure yielding different supramolecular morphologies for the peptide-based BCOs. The α-helical rods tend to arrange as hexagonally packed cylinders, which are assembled into a superstructure due to the phase segregation induced by the coil in combination with aggregation of the rods. Schlaad and coworkers showed the formation of lamellar superstructures using PS-*b*-poly(Z-L-lysine) (PS-*b*-PZLLys) polymers as a result of crystallization by the hexagonally packed PZLLys rods.[138] The thicknesses of the PS and PZLLys phases calculated from the SAXS data vary widely which is a direct result of "breakout" crystallization driven assembly, ignoring the volume fractions of the blocks in the morphology. The authors highlight the importance of dispersity by the formation of a disordered zigzag lamellar structure of a polydisperse BCO. In contrast, the monodisperse analogue with a discrete PZLLys block formed a phase with almost perfect smectic order.

In a similar way, dispersity effects on the morphology of amorphous-crystalline BCOs were observed by Meijer and coworkers using oDMS-*b*-oLLA.[139] The dispersity was varied systematically with the subsequent BCO library allowing the effect of chain length variations in each block to be studied while keeping the composition and DP constant. The bulk oligomers show the formation of a lamellar morphology using SAXS in both discrete and disperse oDMS-*b*-oLLA (Figure 16). Interestingly, the discrete BCO possessed scattering peaks that are very defined while the introduction of a disperse oDMS block resulted in a domain spacing which is 6% larger. Dispersity in the crystalline part (oLLA) has a dramatic effect on the long-range organization. The effect was

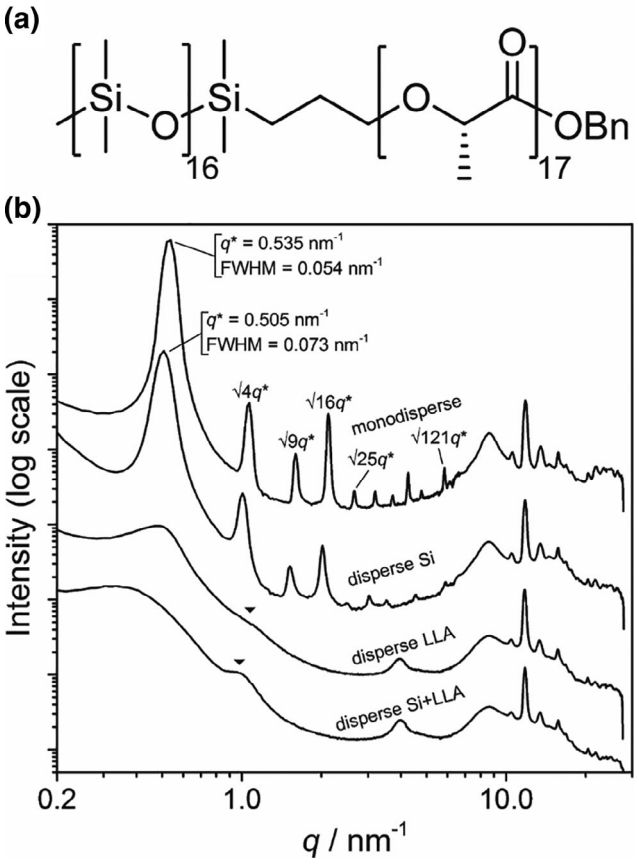

FIGURE 16 (a) Molecular structure of oDMS-*b*-oLLA, (b) SAXS data for discrete and partially disperse oDMS-*b*-oLLA (the broad peak at $q = 4$ nm^{-1} results from background scattering). Reprinted from Reference 140, licensed under CC-BY-NC-ND

attributed to imperfect packing of the oLLA chains due to large chain length variations as a result of crystallization which hampers the formation of a sharp interface between the two phases. It is proposed that crystallization governs the chain alignment of oLLA in the discrete system as well as the disperse case. Near-perfect alignment is possible for discrete oLLA chains and therefore the lamellar domain spacing is constant over macroscopic distances. Later, the same group explored the effect of stereocomplexation in oDMS-*b*-oLA and found less defined lamellar structures as a result of an imbalance between crystallization rate and diffusion kinetics.[117] By reducing the size of the blocks using oligomethylene (oM) chains, very small feature sizes of 5.8 nm were observed for $oDMS_7$-*b*-oM_{33} with a crystalline orthorhombic substructure found in the oM block consistent with linear alkane crystals. Moreover, a more detailed study on triblock co-oligomers allowed for a correlation between the domain sizes and the molecular organization of the blocks.[141] Hence, information on the balance between block volumes, block length, crystallization strength, dispersity and the density of interblock links at the domain boundary was obtained. In particular, the block volumes – classically dictating the morphology of the microphase segregated state – are ignored due to crystallization, yielding lamellar structures, irrespective of the volume fractions of the blocks. Similar results were obtained by Zuckermann and Balsara using discrete peptoid block copolymers with amorphous Nte and crystalline polydecylglycine (Nde) sidechains.[142] As a result of Nde crystallization, lamellar phases are formed and hence the formation of a microphase results from crystallization instead of the interaction parameter between the two blocks. These results show the value that discrete oligomeric materials can provide for understanding the crystallinity of two-component phase segregated systems.

Interestingly, the discrete nature of the amorphous-crystalline BCOs described above allows the point at which no distinction between LC and block copolymer behavior can be made. Typically, these two fields are only discriminated by the molecular weight and dispersity of the respective molecules. The rod-like character of the rigid, crystalline block bridges the gap between LCs and block copolymers further. Using LC molecules with a short (DP $\leq$4), phase segregating coil, permits non-conventional mesophases to be accessed which have been the subject of many reviews.[135,143,144] However in the present review, we focus on the assembly of block molecules with phase segregating, discrete length oligomer coils conjugated to rigid, rod-like or supramolecular blocks.

Periodic structures with nanoscale dimensions can be obtained based on an extended biphenyl core decorated with oligo(propylene oxide) on the periphery shown by Lee and coworkers.[145] The repulsion between the blocks and anisometric shape of the rod segment imparts orientational organization and gives rise to 1-D, 2-D, and 3-D nanostructured assemblies by varying the oligo(propylene oxide) chain length. Another example includes perfluorinated coils in block molecules which are widely used as the phase-segregating segment in LC materials and the mesophases have been extensively studied due to the promising technological applications. Neubert and coworkers showed a striking increase in chemical and thermal stability of the mesophases when a perfluorinated chain is attached to the periphery of a rod.[146] Furthermore, only smectic phases were obtained due to the strong segregation. This feature was also utilized by Marks and coworkers to form highly ordered layers of thiophene oligomers segregated by perfluorohexyl chains with high thermal stability.[147] As a result, reproducible film growth and defect free charge-transport properties were obtained leading to efficient n-type semiconductors. Highly organized films with a low defect density were also be obtained by Schenning and coworkers using a strongly phase segregating oDMS block attached to an azobenzene LC rod (Figure 17).[148] Regardless of the number of siloxane repeating units, columnar structures were observed due to the architecture of the molecular building block. The cylindrical domains could be easily aligned via graphoepitaxy with the resulting sub-5 nm patterns of significant utility for the fabrication of nanopatterned devices.

Building on these LC-systems, materials with well-ordered, switchable morphologies can be obtained where both azobenzene crystallization and oDMS phase segregation drive the morphology, as described by Meijer and coworkers.[149] End functionalization of a discrete oDMS with azobenzene gives monolayers of crystalline

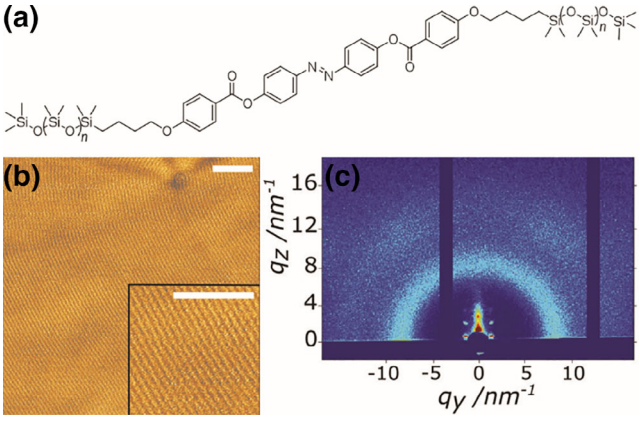

FIGURE 17 (a) Molecular structure of LC-oDMS, (b) tapping mode AFM phase image of LC-22Si, scale bars: 50 nm, (c) grazing incidence XRD data of LC-22Si. Reprinted from Reference 148, licensed under CC-BY-NC

azobenzenes that are exfoliated by the liquid-like siloxane oligomer. Moreover, irradiation with light leads to reversible changes in the physical state of the material from solid to liquid via *trans* to *cis* photoisomerization of azobenzene (365 nm) and *cis* to *trans* isomerization (455 nm). The change in physical state can be attributed to a shift from an ordered lamellar to a disordered state as shown via SAXS. Remarkably, the nature of the end group on the azobenzene segment has a significant impact on material morphology as was observed by exchanging a methoxy with a hydroxy end group, which results in a change from lamellar to a cylindrical morphology, associated with a loss of the crystalline interactions. This illustrates that these oligomers are also sensitive to small changes in structure, giving rise to substantial transformations in the nanoscale morphology. Similar effects were observed for discrete oDMS with ureidopyrimidone or benzyl protected ureidopyrimidone end groups, switching between block copolymer-like and liquid crystalline self-assembly, respectively.[60] The ureidopyrimidone solely segregates from the oDMS forming block copolymer assemblies (lamellar, hexagonal, base cubic centered, or disordered) which could be tailored via the number of DMS repeating units. The introduction of a benzyl protecting group provides a driving force for the ureidopyrimidone end groups to crystallize and only lamellar structures were obtained irrespective of the oDMS volume fraction. Not only ureidopyrimidone and azobenzenes have been utilized for oligomer materials with interesting properties and highly ordered morphologies, also dinitrohydrazones and naphthalenediimides were attached to the periphery of oDMS.[150,151] Effects of polymorphism and molecular architecture on the morphology were observed. The ability to tailor these A-oDMS-A type block molecules has given great insight in the assembly driving forces and properties of rod-like mesogens and supramolecular moieties in a liquid-like matrix. In general, low molecular weight BCOs and decorating LC rods with discrete oligomers has blurred the boundaries between both assembly fields and thus many similarities in assembling properties have been observed. Of particular note, crystallization in competition with phase segregation in block molecules can have a profound influence on the morphology of the materials. Although a range of amorphous–crystalline block combinations have been examined, it remains a challenge to predict the assembly structure from the molecular design with significant future opportunities.

3.3 | Discrete oligomers in solution

Discrete oligomers have been frequently studied in solution and analogous to bulk self-assembly, striking effects of DP, chain ends, and dispersity on the resulting nanostructures have been observed. These features reinforce the power of these fundamental studies in combining solution self-assembly and molecular recognition for future progress in molecular design and applications in, for example, catalysis.

3.3.1 | Self-assembly and molecular recognition

Self-assembly, including molecular recognition, plays a significant role in natural processes where non-covalent interactions guide the folding of proteins and induce the dimerization of DNA into helices. Chemists frequently try to mimic this behavior in synthetic analogs, though this field is still in its infancy when compared to highly evolved biological systems. Discrete oligomers provide an opportunity to study these intramolecular and intermolecular interactions in a systematic manner. This introduces advanced fundamental understanding of length and sequence requirements for the generation of folded and higher-order assembled structures of abiotic materials in solution. In many cases, these processes/interactions cannot be observed with disperse polymers.

The stereocomplex formation of syndiotactic and isotactic poly(methyl methacrylate) leading to a triple helix self-assembled state, was originally observed in 1965.[152] Multiple studies have been dedicated to characterize the overall stoichiometry and composition of the complex. In this process the isotactic PMMA forms a double helix that resides inside a third helix formed from syndiotactic PMMA. In order to determine the specific length requirements needed to elicit this complexation behavior, Hawker and coworkers used a chromatographic approach to generate a series of discrete isotactic oMMA (*it*-oMMA) and syndiotactic oMMA (*st*-oMMA) oligomers from the parent disperse tactic polymers (Figure 18).[153] This generated two libraries of oligomers that could be combined in different ratios to identify the onset of stereocomplex generation, which was found to be a 15-mer for the isotactic component and a 20-mer for the syndiotactic oligomer, *it*-oMMA$_{15}$, and *st*-oMMA$_{20}$, respectively. The formed structure corresponds to the *it* double helix having one and a half helical turns and the *st* helix requiring one full helical turn to productively associate. Additionally, the properties of the oligocomplexes could be tailored via the stoichiometry of the oligomers and their length to change the T_m of the assembly. More interestingly, the assemblies demonstrated selective self-sorting to generate the most thermodynamically stable complexes from the fewest number of components when multiple lengths of oligomers were

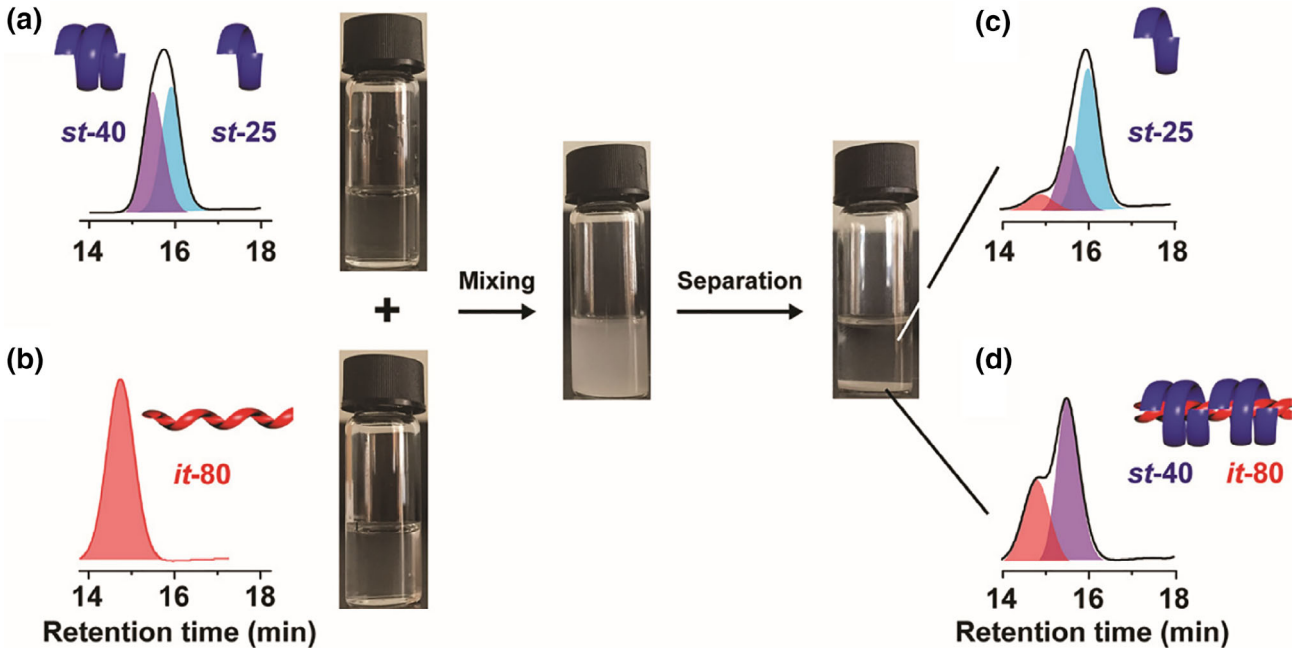

FIGURE 18 Binding selectivity of oMMA toward high molecular weight complementary species: (a) 50:50 wt% mixture of *st*-oMMA$_{25}$ and *st*-oMMA$_{40}$, (b) *it*-oMMA$_{80}$, (c) the supernatant, and (d) the precipitate collected after mixing the initial oMMA solutions (*it*−/*st* molar ratio = 1:4). Reprinted with permission.[153] Copyright 2018, American Chemical Society 2018

present at the same time, similar to DNA. Thus, a mixture of 1 eq. *it*-oMMA$_{80}$, 2 eq. *st*-oMMA$_{40}$, and 2 eq. *st*-oMMA$_{25}$ in acetonitrile predominately gives a complex of *it*-oMMA$_{80}$ and *st*-oMMA$_{40}$ that precipitates from solution, while oMMA$_{25}$ stays in the supernatant. In such a way, molecular design can be utilized to facilitate defined intermolecular interaction in solution.

Another study that targeted for molecular recognition was published by Huc and coworkers, who reported the translation of rod-like templates to assemblies of helical oligomers.[154] Libraries of alkylcarbamate oligomers were prepared as templates with controlled number (from 1 to 4) and distance between carbamate functions (from 3 to 10 methylene units) and control over stereocenters. The templates were complexed with discrete oligo amides forming double helices in solution. After complexation with the template rods, single or double helical host-guest helix-rod complexes were observed and analyzed via NMR, CD spectroscopy, X-ray crystallography and ion mobility mass spectrometry. Most notably, molecular sorting was observed that was induced via chiral rod-helix and chiral helix–helix interactions. Finally, the helices could be aligned in an organized sequence on the template rod. Such structure formation relies on the precision with which the utilized oligomers could be prepared, as the underlying interactions greatly depend on the specific number of repeating units and the distance between the interacting functional groups.

Prior to these studies, Moore and coworkers pioneered the concept of well-defined folding of oligomers in solution.[155] In these discrete systems, phenylacetylene oligomers were observed to form foldamers with a helical conformation and a large cavity in solution. By controlling the dimensions of this cavity, the foldamer could be utilized to specifically associate with chiral molecules.[156] Therefore, a *m*-phenylethylene oligomer was utilized to form complexes with chiral monoterpenes. The binding between foldamer and monoterpene depended significantly on substituents on the oligomer backbone and the overall number of repeat units.

Oligomer materials can also lead to novel aggregation behavior in solution, covering the formation of micelles, vesicles, or more complex structures with high precision. Such structures are especially useful for applications such as cargo delivery, nanoreactors or catalysis. Although disperse BCOs feature a variety of useful properties and unprecedented aggregation behavior,[157–160] significantly enhanced properties can be obtained from partially or fully discrete BCOs. For example, a combination of discrete and disperse blocks was utilized by Hawker and coworkers in the study of directed self-assembly via metal ion coordination in amphiphilic BCOs.[161] A discrete

oligo(histidine) block was coupled to a synthetic oligostyrene to give BCOs that formed vesicles in aqueous buffer. The addition of divalent ions led to the formation of assembled structures that was dependent on the metal used. Aggregated micelles were observed with addition of Zn^{2+}, Co^{2+}, or Cu^{2+}, while multilamellar vesicles were obtained with Mn^{2+} and isolated micelles with Ni^{2+} and Cd^{2+}. The change in the morphologies was attributed the geometry of the complex in addition to the nature of the transition metal. Tetrahedral and square planar complexes led to aggregated micelles, while octahedral complexes afforded isolated micelles. Similarly, a BCO based on a discrete oligosaccharide and PNIPAM was described by Borsali and coworkers[162] with the discrete oligosaccharide building block being prepared via ring-opening of ß-cyclodextrin to give maltoheptaose. The oligosaccharide was then monofunctionalized with an alkyne followed by conjugation with disperse PNIPAM to give vesicular structures with diameters around 300 nm when heated above the lower critical solution temperature of the PNIPAM block.

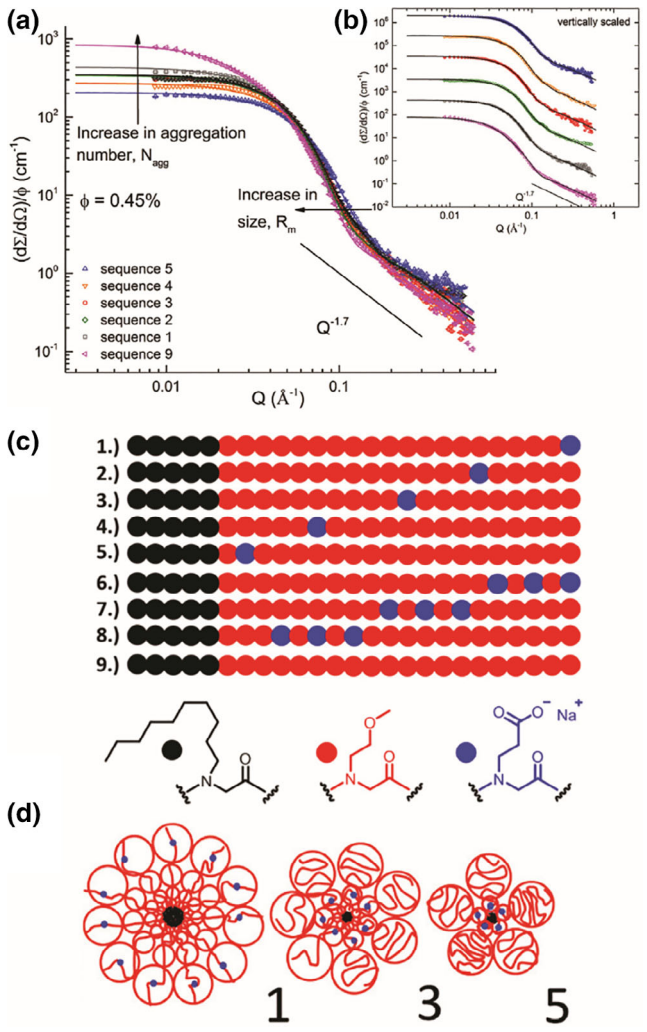

FIGURE 19 Self-assembly of amphiphilic BCOs: (a) SANS scattering intensity, normalized by the polymer volume fraction and analysis of the micellar solutions of sequence-defined peptoid block copolymers bearing a single ionic monomer (b) the data vertically scaled, (c) chemical structures of representative sequences of ionic peptoid block copolymers, (d) a cartoon representation of the micellar structure with respect to the ionic monomer position along the peptoid polymer chain. Reprinted with permission.[163] Copyright 2018, American Chemical Society 2018

The self-assembly behavior of discrete amphiphilic peptoid BCOs in aqueous solution has also been studied by John, Schneider and Zhang leading to spherical micelles in the size range of 5–10 nm (Figure 19).[163] Ionic repeat units were incorporated at specific points along the oligomer backbone allowing the effect of sequence variations on self-assembly to be studied. As shown using SANS, the size of micelles and the aggregation number increased with distance of the ionic repeat unit from the hydrophobic block. In addition, the micelle size was shown to systematically change due to the driving force of the system to minimize electrostatic repulsion. An enhanced effect was observed when the number of ionic repeat units was increased and placed in different positions along the backbone.

Meijer and coworkers investigated the effect of dispersity on crystallization driven self-assembly in aqueous solution (Figure 20).[164] An amphiphilic ABA BCO was synthesized with oEG outer blocks and an oLLA inner block. Moreover, the synthetic strategy allows the effect of succinic acid and methyl ether end functionalities to be probed. In the case of methyl ether end functionalization, cylindrical micelles were observed forming thin fibers for a discrete sample and bundles of fibers for a disperse sample. After heating and cooling to ambient temperature the discrete sample formed a gel, while no gelation was observed for the disperse sample. In contrast, for succinic acid functionalized derivatives, uniform sheets were observed for the discrete species, while a mixture of structures was observed for the disperse sample. The significant difference of discrete and disperse BCOs was attributed to the enhanced crystallinity of the discrete oLLA block. This study further demonstrates the role of end groups in influencing the morphologies obtained. Recently, a more detailed understanding of the oEG-*b*-oLLA system toward the formation of spherical micelles, cylindrical micelles and vesicles was achieved.[165] Significantly, the formed structures could be tailored via the individual block length and were predictable via self-consistent field computations. Furthermore, the effect of LA block crystallinity on solution self-assembly of amphiphilic oEG-*b*-oLA was investigated.[166]

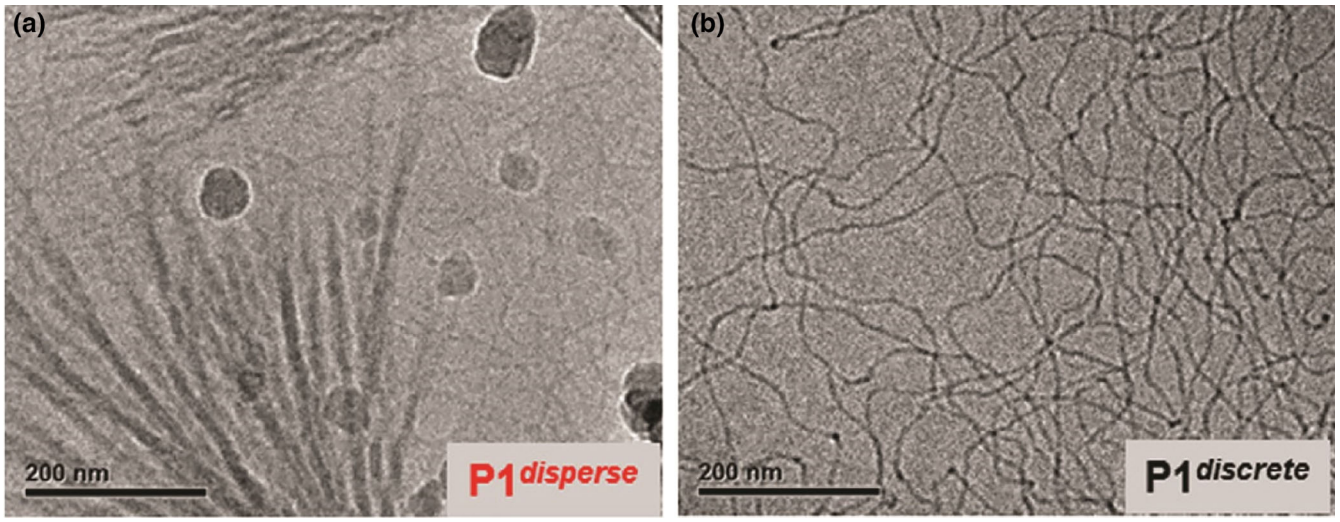

FIGURE 20 Self-assembly of amphiphilic oEG-*b*-oLLA: (a) cryo TEM images of disperse oEG-*b*-oLLA and (b) cryo TEM images of discrete oEG-*b*-oLLA.Reprinted from Reference 164. Licensed under CC-BY-NC-ND

3.3.2 | Catalysis and interactions with the environment

While the fundamental properties of oligomer-based self-assemblies in solution provide insight into structure–property relationships, studies regarding applications in catalysis and interaction with the environment have been performed as well. The combination of precise oligomers and catalytically active molecular species is an effective way to improve catalyst activity and selectivity. As catalytic processes are governed to a large extent by the orientation of catalyst and substrate, control over the nanoenvironment provided by discrete oligomers is very useful for enhancing catalyst performance. Discrete, catalytically active oligomers based on peptoids were presented by Kirshenbaum and coworkers.[167] Inclusion of 2,2,6,6-tetramethyl-1-piperidinyloxyl (TEMPO) into a phenylethylamine-based helical peptoid backbone at specific points of the chain and the stereochemical configuration of the phenylethylamine monomer was varied to modulate and study the effect of stereochemistry on catalytic activity in the oxidative kinetic resolution of racemic secondary alcohols. The catalyst activity was optimized according to placement of the TEMPO unit along the backbone for steric access with dramatic sequence dependence being observed. Enantiomeric excesses of the synthesized peptoids ranging from 5% to 99% were found to be dependent on the steric environment for optimized systems.

Similarly, Fernandes and coworkers utilized sequence defined oligomers for catalytic purposes (Figure 21).[168] In this study, a tailored catalytically active trimer was synthesized and grafted on mesoporous silica particles with the pyridyl triazole Cu/TEMPO/*N*-methyl imidazole catalyzed aerobic oxidation of alcohols performed as a model reaction. Iterative CuAAc was employed to form a library of trimers with defined sequences and a trimer with random sequence was synthesized as a reference. A five-fold increase of reactivity was observed for the ideal sequence oligomer, illustrating that accessibility of the individual catalytic centers is more selective regarding the substrate molecule and can be optimized according to the reaction pathway, potentially due to optimized packing of the oligomers on the silica surface.

This selective interaction with surfaces was more clearly demonstrated by Gibson and coworkers who described the effect of oligo(vinyl alcohol) (oVA) on the inhibition of ice crystallization. Acting as an anti-freeze protein mimic,[106] the oVA derivatives were prepared via RAFT polymerization and the oligomeric mixture separated via column chromatography in order to evaluate the effect of size and dispersity on ice recrystallization. At first it was observed that the disperse higher molecular weight oligomer had an improved recrystallization inhibition compared to discrete molecular weight oligomers. However, the study revealed the critical number of repeating units for biomimetic ice recrystallization inhibition in which a "switch on" at 12 repeating units of VA was observed. These insights are key for the design of improved ice recrystallization inhibition additives that are required for tissue and cell storage applications.

Whittaker and coworkers synthesized discrete trifluoroethyl end functionalized oligo(acrylic acid) (oAA) via chromatographic purification for potential use as ^{19}F MR imaging agents in biomedical diagnostics.[169] A strong relationship between the number of repeating units and dispersity on magnetic resonance properties was observed via ^{19}F NMR relaxation studies and ^{19}F

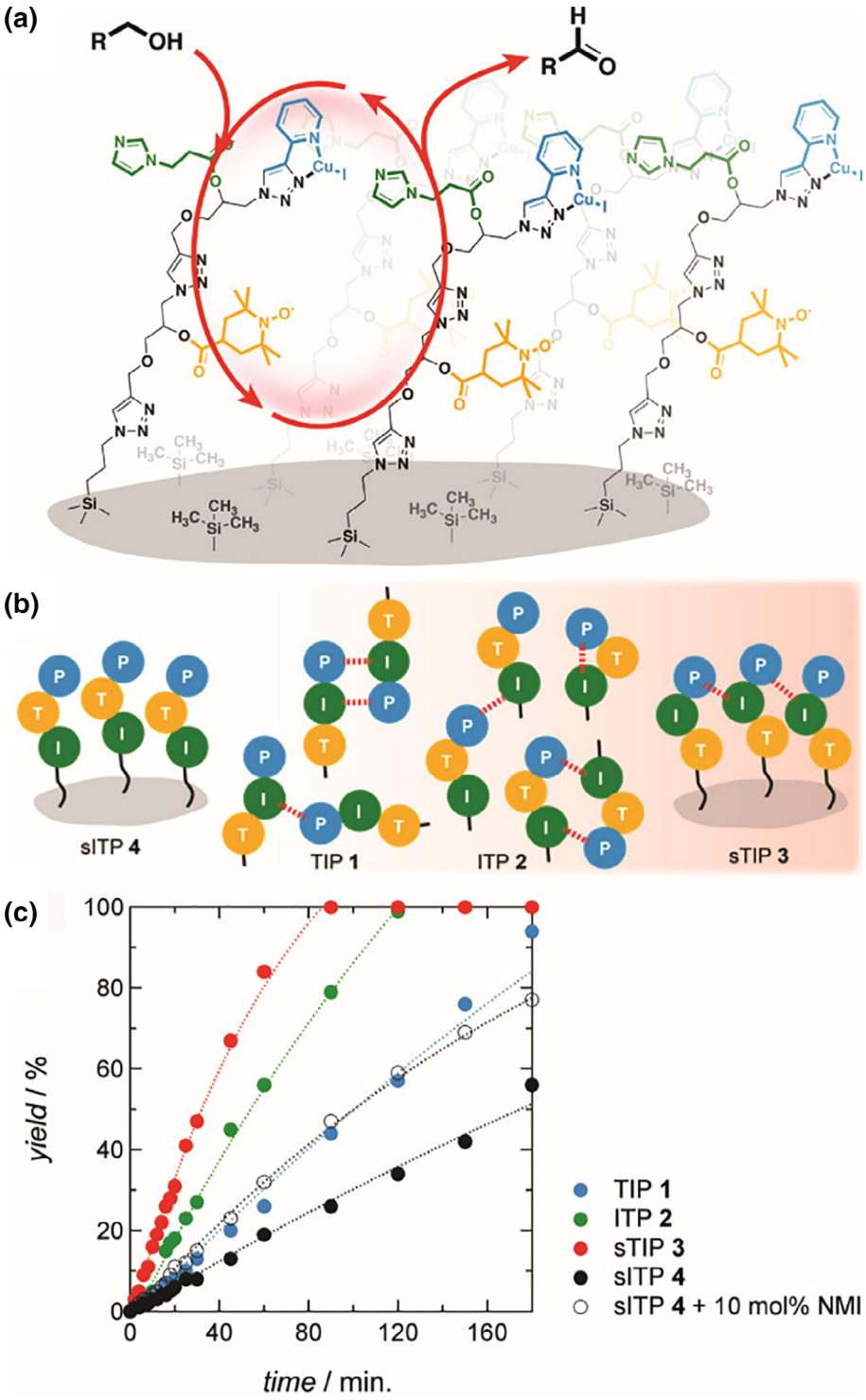

FIGURE 21 (a) Schematic overview over the catalytic reaction pathway, (b) view of cooperative interactions in soluble and supported sequence-defined catalytic oligomers and (c) catalytic activity of TIP, ITP, sTIP, and sITP in the aerobic oxidation of benzyl alcohol. Reprinted with permission.[168] Copyright 2018, American Chemical Society

magnetic resonance imaging (MRI). With an increasing number of repeating units or chain length, the ^{19}F MRI signal-to-noise ratio was observed to increase and the T_1 relaxation time decrease. This ability to tune in molecular dynamics of the ^{19}F probes via oligomer length translated into improved imaging capability. Moreover, an enhanced signal-to-noise ratio was observed in the case of discrete oligomers versus the corresponding disperse materials.

The combination of living polymerization and chromatographic separation was also employed by Hoshino and coworkers while studying the molecular recognition of the peptide melittin by synthetic oligomers.[108] A library of discrete BCOs consisting of oAA (deprotection of oTBA) and oNIPAM blocks was synthesized via RAFT and chromatography purification. In the next step, an aggregation essay was performed to investigate interactions with melittin to identify recognition according to

oligomer length and block length ratio. Moreover, peptides with different epitope sequences were probed in order to elucidate the specificity of peptide/oligomer interaction. The authors showed that tailored oligomer synthesis can lead to significant specificity in peptide recognition with potential future applications for neutralizing (toxic) biological activity.

3.3.3 | Conjugated oligomers in solution

Conjugated polymers play a significant role in contemporary polymer science and they represent one of the most actively studied oligomer classes.[25,170] This interest is driven by the strong dependence of conjugated structures on the number of repeating units, as this directly correlates to the potential degree of conjugation. As a result, discrete oligomers present the opportunity to prepare libraries that precisely tune the wavelength of light absorption and emission. Recent contributions are discussed below with the reader being referred to prior reviews and references.[25,28,29]

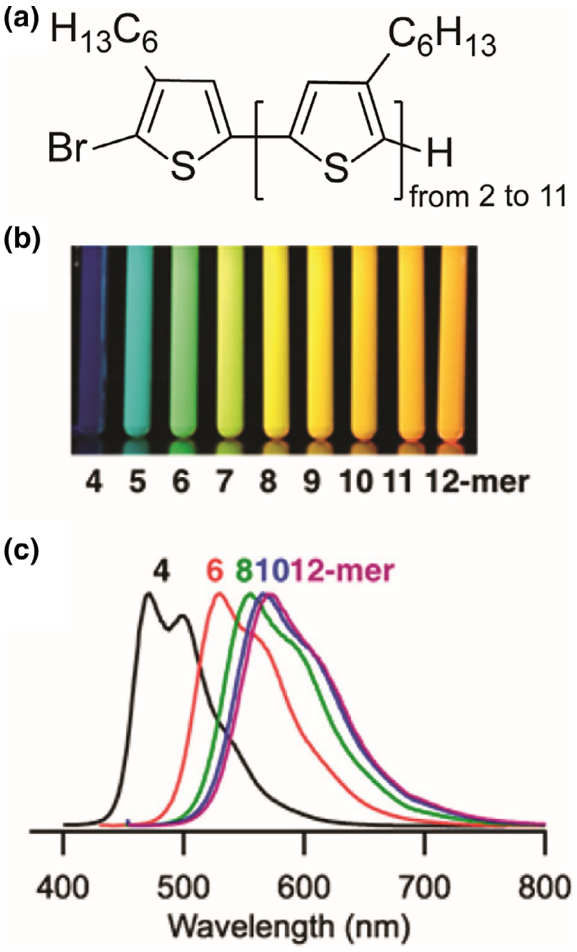

FIGURE 22 Optical properties of conjugated oligomers in solution: (a) structure of discrete o3HTs, (b) photograph of the discrete o3HT series tetramer to dodecamer under 365 nm UV light and (c) PL emission spectra of the discrete o3HT series tetramer to dodecamer. Reprinted with permission.[105] Copyright 2018, American Chemical Society

Hawker and coworkers synthesized o3HT libraries with repeating units ranging from 4 to 18 via chromatographic separation (Figure 22).[105,116] Discrete oligomers with distinct optical properties were obtained, and the expected red-shift in absorption maxima and emission maxima observed with increasing number of repeat units due to the increased conjugation length. To illustrate the significant difference between ensemble properties and molecular properties, a comparison between disperse and discrete oligomer samples showed a change in emission properties from yellow for a disperse hexamer mixture to green for the discrete hexamer. A combination of oligomers with various numbers of repeating units permitted formation of blends with white light emission. In addition, the concept was extended toward other conjugated oligomers, such as oligo(fluorenes) or copolymers with benzothiadiazoles placed at different locations along the oligomer backbones. These results are in good agreement with earlier studies in which the free rotation of the single bond in π-conjugated oligomers gives rise to a saturation in conjugation with a linear relationship between band gap and 1/n. Zhu and coworkers described monodisperse π-conjugated fluorene oligomers with azo units in the main chain.[171] The isomerization wavelength of the azo group was shifted into the visible light via the conjugation length. Interestingly, the photoisomerization took place only at one end of the oligomer, which was also supported by DFT modeling.

A study that made use of iterative synthesis was conducted by Stuparu and coworkers, who examined the photophysical properties of discrete π-conjugated oligomers formed from planar and nonplanar aromatic moieties (Figure 23).[172] Corannulene and thiophene were combined with an alkyne-bridge via Sonogashira coupling in an alternating fashion to give discrete oligomers that featured excellent electronic properties. As the absorption behavior suggested, the bridged corannulene and thiophene moieties structures formed a non-planar π-conjugated system. Interestingly, longer oligomers showed nonlinear absorption and emission properties including two-photon absorption and luminescence. These studies exemplify that sequence specificity, namely alternating order, has a significant effect on electronic properties with contributions from a combination of different geometries, that is, nonlinear optical properties. PPVs conjugated to PNIPAM have also been utilized by Huang and coworkers for the formation of self-assembled

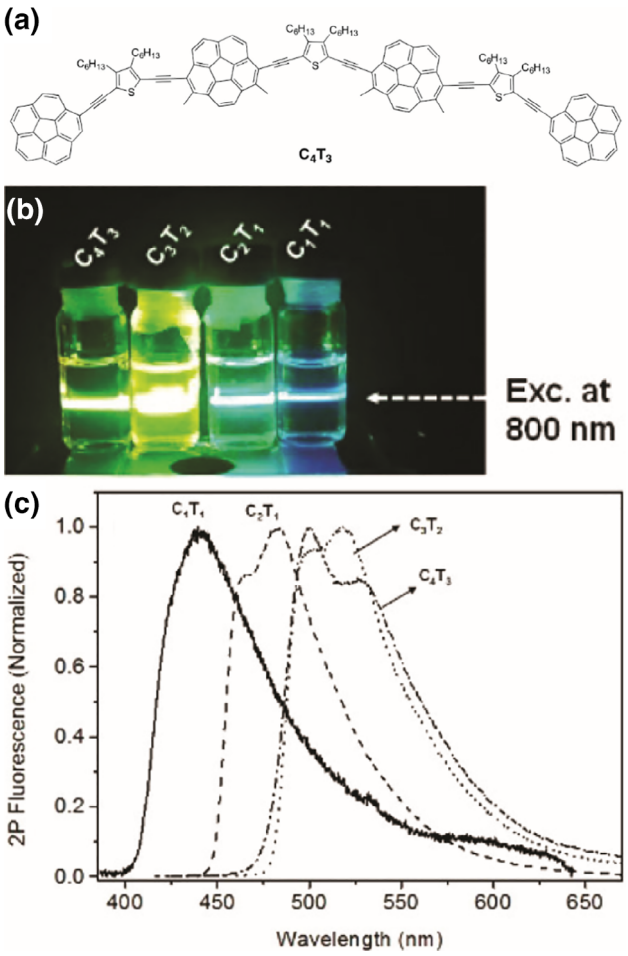

FIGURE 23 (a) Structure of corannulene and thiophene oligomer C_4T_3, (b) photograph showing two-photon excited emission from corannulene and thiophene oligomers excited with 800 nm femtosecond laser, and (c) two-photon excited emission of from corannulene and thiophene oligomers in $CHCl_3$. Reprinted with permission.[172] Copyright 2017, American Chemical Society 2017

fibers in ethanol.[173] Crystallization driven self-assembly of the oPPV block was observed via a self-seeding or seeded growth process to give monodisperse fiber-like micelles with widths of 22 nm and lengths up to 870 nm. Notably, other polymers, namely poly(2-(diethylamino) ethyl methacrylate (PDEAEMA), could be conjugated to the oPPV core as well. PDEAEMA-based fiber-like micelles could also be formed and subsequently utilized as a seed to form triblock comicelles after addition of oPPV-*b*-PNIPAM unimers. Overall, the crystallizing oligomer acts as structure directing agent, while the polymer drives solubility and provides a bulky corona to stabilize nanostructures. The combination of PPV monomers and benzothiadiazole monomers was investigated by Meyer and coworkers[174] with the combination of donor and acceptor repeat units in a sequence specific manner leading to unprecedented optical properties directly related to the starting molecular structure. Similarly, absorption and redox potentials could be tailored, for example, a shift in the absorption maximum of 19 nm or in the electrochemical oxidation potential of 0.17 V. Moreover, bulk heterojunction solar cells fabricated from these sequence-controlled oligomers result in power conversion efficiencies varying by a factor of three depending on monomer sequence with the highest efficiency for the alternating oligomer.

The utilization of conjugated repeat units for analysis of metal complex-based supramolecular self-healing materials was presented by Hager and coworkers.[175] An oligomeric π-conjugated fluorescence marker was synthesized that can insert into the supramolecular self-healing network via complexation with Zn^{2+}. Scratches in the supramolecular network leads to decreased fluorescence due to debonding of Zn^{2+}-marker complexes. The return of fluorescence intensity was measured over time to evaluate self-healing progress. This allows self-healing efficiency to be investigated as a direct readout from the system on a molecular scale. Effective self-healing analysis is due to the fluorescent properties of the oligomers and a similar mobility of the oligomer compared to polymer chains in the network during the self-healing step. Molecular orientation was also investigated by Chujo and coworkers who prepared conjugated planar-chiral oligomers based on [2.2]paracyclophanes with both twisted and cyclic oligomers studied.[176] Interestingly, photoexcitation led to similar photophysical properties suggesting folding of the twisted oligomer into a cyclic structure, resembling a helix. The folding can be attributed to the flexibility of the oligomer that allows folding into a planar cyclic structure. Moreover, an intense chiral photoluminescence with high quantum efficiency was observed, which is a promising feature for the fabrication of chiral scaffolds.

4 | CONCLUSIONS AND OUTLOOK

Oligomer research or macro-organic chemistry is an emerging area of focus driven by molecular sizes between traditional small molecule and polymer systems. Combined with the ability to prepare discrete or very low dispersity samples, oligomers have significant potential for the development of optimized materials in next-generation applications and for fundamental structure property relationships. While great strides have been made to synthesize well-defined oligomers, additional challenges need to be addressed for translation from basic science to practical applications. Approaches to oligomer preparation through iterative synthesis allow access to

discrete materials but rarely in significant quantities, while this is partially addressed by the combination of controlled synthesis and purification strategies, improvements are still required. Innovations such as the system developed by Leibfarth and coworkers to automate the synthesis of precision oligomers in flow is an excellent example of novel approaches to resolve the issue of scalability.[114] Additionally, more attention should be devoted to studying chain end effects for discrete oligomeric materials, which are far from negligible given the moderate size of oligomeric molecules.

Molecular recognition of oligomers will continue to be a research focus with significant inspiration from biological systems such as oligosaccharides. The elucidation and optimization of molecular recognition is a challenging endeavor, and the accumulated knowledge from saccharide- and peptide-based recognition and related techniques will be invaluable. In addition to the recognition of abiotic oligomers with biological systems, the role in small molecule substrate binding to effect catalytic reactions with exquisite selectivity is an opportunity that has tremendous potential. Recent studies have shown the significant effect that oligomer structure and sequence can have on catalytic properties and it is expected that more complex reactions and multi-functional oligomer designs will be developed in the future. Sequence defined oligomers are also expected to be valuable in the developing area of information storage, which requires well-defined oligomers to correlate molecular structure with the storage of information at ultra-high densities.[35,177]

Looking to the future, there are a wide range of exciting directions for discrete and well-defined oligomeric materials. From the perspective of structure, the parameters of length, composition, stereochemistry, and dispersity have all been shown to play a direct role in tuning final materials properties. For chemical composition, one can easily see opportunities for oligomeric analogs of classical polymeric materials (vinyl polymers, ring-opening materials, etc.) being explored further with the techniques described above. The effect of dispersity is frequently observed in these systems but may not be a desirable feature depending on the application. One avenue that has been neglected is oligomer architecture with the investigation of cyclic, star or miktoarm star oligomers showing significant potential for new nanostructures in solution self-assembly or thin films. A true bottleneck that will need to be addressed is how to properly optimize a system with so many parameters and, if vast libraries of materials are generated exploring this chemical space, how to properly evaluate and test them in a reasonable timeframe. This challenge of high throughput materials screening is particularly relevant for oligomer research and advances with oligomers may simplify more complex, higher molecular weights polymers and macromolecular architectures.[178]

ACKNOWLEDGMENTS

This work is financed by the Royal Netherlands Academy of Arts and Sciences and the Dutch Ministry of Education, Culture and Science (Gravity program 024.001.035) (BvG, BAG, EWM). WRG thanks Georgia Institute of Technology for start-up funding. BS thanks the Max-Planck-Society and the University of Glasgow for funding. The U.S. Army Research Office under Cooperative Agreement W911NF-19-2-0026 for the Institute for Collaborative Biotechnologies is acknowledged for support (CJH). Bas van Genabeek and Brigitte A. G. Lamers contributed equally to this work.

ORCID

Bas van Genabeek https://orcid.org/0000-0002-4516-4469
Brigitte A. G. Lamers https://orcid.org/0000-0002-3312-8962
Craig J. Hawker https://orcid.org/0000-0001-9951-851X
E. W. Meijer https://orcid.org/0000-0002-4130-3775
Will R. Gutekunst https://orcid.org/0000-0002-2427-4431
Bernhard V. K. J. Schmidt https://orcid.org/0000-0002-3580-7053

REFERENCES

[1] A. D. Jenkins, P. Kratochvíl, R. F. T. Stepto, U. W. Suter, *Pure Appl. Chem.* **1996**, *68*, 2287.
[2] A. Varki, *Glycobiology* **1993**, *3*, 97.
[3] G. R. Luckhurst, *Macromol. Symp.* **1995**, *96*, 1.
[4] V. Percec, M. Kawasumi, *Macromolecules* **1992**, *25*, 3843.
[5] C. J. Hawker, J. M. J. Frechet, *J. Am. Chem. Soc.* **1990**, *112*, 7638.
[6] J. S. Moore, *Acc. Chem. Res.* **1997**, *30*, 402.
[7] U. Scherf, K. Müllen, *Synthesis* **1992**, *1992*, 23.
[8] S. Zalipsky, *Bioconjugate Chem.* **1993**, *4*, 296.
[9] D. S. Breslow, *Prog. Polym. Sci.* **1993**, *18*, 1141.
[10] R. Scott Lokey, B. L. Iverson, *Nature* **1995**, *375*, 303.
[11] J.-F. Lutz, M. Ouchi, D. R. Liu, M. Sawamoto, *Science* **2013**, *341*, 1238149.
[12] B. V. K. J. Schmidt, C. Barner-Kowollik, *Nat. Chem.* **2013**, *5*, 990.
[13] S. C. Solleder, R. V. Schneider, K. S. Wetzel, A. C. Boukis, M. A. R. Meier, *Macromol. Rapid Commun.* **2017**, *38*, 1600711.
[14] E. Ruoslahti, M. Pierschbacher, *Science* **1987**, *238*, 491.
[15] M. D. Pierschbacher, J. W. Polarek, W. S. Craig, J. F. Tschopp, N. J. Sipes, J. R. Harper, *J. Cell. Biochem.* **1994**, *56*, 150.
[16] J. Goodchild, *Bioconjugate Chem.* **1990**, *1*, 165.
[17] V. K. Sharma, J. K. Watts, *Future Med. Chem.* **2015**, *7*, 2221.
[18] P. H. Seeberger, D. B. Werz, *Nature* **2007**, *446*, 1046.

[19] K. L. Wooley, C. J. Hawker, J. M. J. Fréchet, *Angew. Chem., Int. Ed.* **1994**, *33*, 82.

[20] K. L. Wooley, C. J. Hawker, J. M. Pochan, J. M. J. Frechet, *Macromolecules* **1993**, *26*, 1514.

[21] B. Pan, D. Cui, Y. Sheng, C. Ozkan, F. Gao, R. He, Q. Li, P. Xu, T. Huang, *Cancer Res.* **2007**, *67*, 8156.

[22] R. Zana, *Adv. Colloid Interface Sci.* **2002**, *97*, 205.

[23] A. Laschewsky, L. Wattebled, M. Arotçaréna, J.-L. Habib-Jiwan, R. H. Rakotoaly, *Langmuir* **2005**, *21*, 7170.

[24] F. Wang, A. Klaikherd, S. Thayumanavan, *J. Am. Chem. Soc.* **2011**, *133*, 13496.

[25] R. E. Martin, F. Diederich, *Angew. Chem., Int. Ed.* **1999**, *38*, 1350.

[26] B. Kirtman, B. Champagne, *Int. Rev. Phys. Chem.* **1997**, *16*, 389.

[27] N. S. Sariciftci, *Primary Photoexcitations in Conjugated Polymers: Molecular Exciton Versus Semiconductor Band Model*. Singapore: World Scientific, **1998**.

[28] S. S. Zade, N. Zamoshchik, M. Bendikov, *Acc. Chem. Res.* **2011**, *44*, 14.

[29] A. L. Kanibolotsky, I. F. Perepichka, P. J. Skabara, *Chem. Soc. Rev.* **2010**, *39*, 2695.

[30] S. Binauld, D. Damiron, L. A. Connal, C. J. Hawker, E. Drockenmuller, *Macromol. Rapid Commun.* **2011**, *32*, 147.

[31] R. B. Merrifield, *J. Am. Chem. Soc.* **1963**, *85*, 2149.

[32] M. Porel, C. A. Alabi, *J. Am. Chem. Soc.* **2014**, *136*, 13162.

[33] S. Pfeifer, Z. Zarafshani, N. Badi, J.-F. Lutz, *J. Am. Chem. Soc.* **2009**, *131*, 9195.

[34] B. L. Bray, *Nat. Rev. Drug Discovery* **2003**, *2*, 587.

[35] R. K. Roy, A. Meszynska, C. Laure, L. Charles, C. Verchin, J.-F. Lutz, *Nat. Commun.* **2015**, *6*, 7237.

[36] A. Al Ouahabi, L. Charles, J.-F. Lutz, *J. Am. Chem. Soc.* **2015**, *137*, 5629.

[37] A. Al Ouahabi, M. Kotera, L. Charles, J.-F. Lutz, *ACS Macro Lett.* **2015**, *4*, 1077.

[38] T. Trinh Thanh, L. Oswald, D. Chan-Seng, J. F. Lutz, *Macromol. Rapid Commun.* **2014**, *35*, 141.

[39] D. Chan-Seng, J.-F. Lutz, *ACS Macro Lett.* **2014**, *3*, 291.

[40] T. Trinh Thanh, L. Oswald, D. Chan-Seng, L. Charles, J. F. Lutz, *Chem. – Eur. J.* **2015**, *21*, 11961.

[41] M. Landa, M. Kotera, J.-S. Remy, N. Badi, *Eur. Polym. J.* **2016**, *84*, 338.

[42] S. Martens, J. Van den Begin, A. Madder, F. E. Du Prez, P. Espeel, *J. Am. Chem. Soc.* **2016**, *138*, 14182.

[43] S. Celasun, F. E. Du Prez, H. G. Börner, *Macromol. Rapid Commun.* **2017**, *38*, 1700688.

[44] C. Yang, J. P. Flynn, J. Niu, *Angew. Chem., Int. Ed.* **2018**, *57*, 16194.

[45] L. Kanasty Rosemary, J. Vegas Arturo, M. Ceo Luke, M. Maier, K. Charisse, K. Nair Jayaprakash, R. Langer, G. Anderson Daniel, *Angew. Chem., Int. Ed.* **2016**, *55*, 9529.

[46] D. Niculescu-Duvaz, J. Getaz, C. J. Springer, *Bioconjugate Chem.* **2008**, *19*, 973.

[47] H. Zhang, X. Li, Q. Shi, Y. Li, G. Xia, L. Chen, Z. Yang, Z. X. Jiang, *Angew. Chem., Int. Ed.* **2015**, *54*, 3763.

[48] Y. Li, X. Qiu, Z.-X. Jiang, *Org. Process Res. Dev.* **2015**, *19*, 800.

[49] S. C. Solleder, K. S. Wetzel, M. A. R. Meier, *Polym. Chem.* **2015**, *6*, 3201.

[50] Y.-H. Wu, J. Zhang, F.-S. Du, Z.-C. Li, *ACS Macro Lett.* **2017**, *6*, 1398.

[51] W. Konrad, F. R. Bloesser, K. S. Wetzel, A. C. Boukis, M. A. R. Meier, C. Barner-Kowollik, *Chem. – Eur. J.* **2018**, *24*, 3413.

[52] B. Zhao, Z. Gao, Y. Zheng, C. Gao, *J. Am. Chem. Soc.* **2019**, *141*, 4541.

[53] J. Xu, C. Fu, S. Shanmugam, J. Hawker Craig, G. Moad, C. Boyer, *Angew. Chem., Int. Ed.* **2016**, *56*, 8376.

[54] C. Fu, Z. Huang, C. J. Hawker, G. Moad, J. Xu, C. Boyer, *Polym. Chem.* **2017**, *8*, 4637.

[55] B. N. Norris, T. Pan, T. Y. Meyer, *Org. Lett.* **2010**, *12*, 5514.

[56] G. R. McKeown, S. Ye, S. Cheng, D. S. Seferos, *J. Am. Chem. Soc.* **2019**, *141*, 17053.

[57] K. Matsumoto, S. Shimada, K. Sato, *Chem. – Eur. J.* **2019**, *25*, 920.

[58] B. van Genabeek, B. F. M. de Waal, M. M. J. Gosens, L. M. Pitet, A. R. A. Palmans, E. W. Meijer, *J. Am. Chem. Soc.* **2016**, *138*, 4210.

[59] B. A. G. Lamers, B. F. M. de Waal, E. W. Meijer, *J. Polym. Sci.* **2020**. https://doi.org/10.1002/pol.20200649.

[60] R. H. Zha, B. F. M. de Waal, M. Lutz, A. J. P. Teunissen, E. W. Meijer, *J. Am. Chem. Soc.* **2016**, *138*, 5693.

[61] K. Matsumoto, Y. Oba, Y. Nakajima, S. Shimada, K. Sato, *Angew. Chem., Int. Ed.* **2018**, *57*, 4637.

[62] Z. Huang, N. Corrigan, S. Lin, C. Boyer, J. Xu, *J. Polym. Sci., Part A: Polym. Chem.* **2019**, *57*, 1947.

[63] M. Van De Walle, K. De Bruycker, T. Junkers, J. P. Blinco, C. Barner-Kowollik, *ChemPhotoChem* **2019**, *3*, 225.

[64] M. N. Holerca, M. Peterca, B. E. Partridge, Q. Xiao, G. Lligadas, M. J. Monteiro, V. Percec, *J. Am. Chem. Soc.* **2020**, *142*, 15265.

[65] W. H. Carothers, J. W. Hill, J. E. Kirby, R. A. Jacobson, *J. Am. Chem. Soc.* **1930**, *52*, 5279.

[66] A. K. Doolittle, R. H. Peterson, *J. Am. Chem. Soc.* **1951**, *73*, 2145.

[67] S. Lee Kwang, G. Wegner, *Makromol. Chem., Rapid Commun.* **1985**, *6*, 203.

[68] G. Ställberg, S. Ställberg-Stenhagen, E. Stenhagen, *Acta Chem. Scand.* **1952**, *6*, 313.

[69] R. R. Reinhard, J. A. Dixon, *J. Org. Chem.* **1965**, *30*, 1450.

[70] G. Ungar, J. Stejny, A. Keller, I. Bidd, M. C. Whiting, *Science* **1985**, *229*, 386.

[71] I. Bidd, M. C. Whiting, *J. Chem. Soc., Chem. Commun.* **1985**, 543.

[72] O. I. Paynter, D. J. Simmonds, M. C. Whiting, *J. Chem. Soc., Chem. Commun.* **1982**, 1165.

[73] G. M. Brooke, S. Burnett, S. Mohammed, D. Proctor, M. C. Whiting, *J. Chem. Soc., Perkin Trans. 1* **1996**, 1635.

[74] G. M. Brooke, C. Farren, A. Harden, M. C. Whiting, *Polymer* **2001**, *42*, 2777.

[75] D. Lengweiler Urs, G. Fritz Monica, D. Seebach, *Helv. Chim. Acta* **1996**, *79*, 670.

[76] K. Takizawa, C. Tang, C. J. Hawker, *J. Am. Chem. Soc.* **2008**, *130*, 1718.

[77] K. Takizawa, H. Nulwala, J. Hu, K. Yoshinaga, J. Hawker Craig, *Polym. Chem.* **2008**, *46*, 5977.

[78] J. B. Williams, T. M. Chapman, D. M. Hercules, *Macromolecules* **2003**, *36*, 3898.

[79] G. M. Brooke, S. Mohammed, M. C. Whiting, *J. Chem. Soc., Perkin Trans. 1* **1997**, 3371.

[80] G. M. Brooke, J. A. Hugh MacBride, S. Mohammed, M. C. Whiting, *Polymer* **2000**, *41*, 6457.

[81] J. M. Lee, M. B. Koo, S. W. Lee, H. Lee, J. Kwon, Y. H. Shim, S. Y. Kim, K. T. Kim, *Nat. Commun.* **2020**, *11*, 56.

[82] M. B. Koo, S. W. Lee, J. M. Lee, K. T. Kim, *J. Am. Chem. Soc.* **2020**, *142*, 14028.

[83] R. Haag, F. Kratz, *Angew. Chem., Int. Ed.* **2006**, *45*, 1198.

[84] R. Fordyce, H. Hibbert, *J. Am. Chem. Soc.* **1939**, *61*, 1910.

[85] S. A. Ahmed, M. Tanaka, *J. Org. Chem.* **2006**, *71*, 9884.

[86] F. A. Loiseau, K. K. Hii, A. M. Hill, *J. Org. Chem.* **2004**, *69*, 639.

[87] A. C. French, A. L. Thompson, B. G. Davis, *Angew. Chem., Int. Ed.* **2009**, *48*, 1248.

[88] Y. Jiang, M. R. Golder, H. V. T. Nguyen, Y. Wang, M. Zhong, J. C. Barnes, D. J. C. Ehrlich, J. A. Johnson, *J. Am. Chem. Soc.* **2016**, *138*, 9369.

[89] J. C. Barnes, D. J. C. Ehrlich, A. X. Gao, F. A. Leibfarth, Y. Jiang, E. Zhou, T. F. Jamison, J. A. Johnson, *Nat. Chem.* **2015**, *7*, 810.

[90] J. Li, M. Leclercq, M. Fossepré, M. Surin, K. Glinel, A. M. Jonas, A. E. Fernandes, *Polym. Chem.* **2020**, *11*, 4040.

[91] Z. Huang, J. Zhao, Z. Wang, F. Meng, K. Ding, X. Pan, N. Zhou, X. Li, Z. Zhang, X. Zhu, *Angew. Chem., Int. Ed.* **2017**, *56*, 13612.

[92] D. L. Pearson, J. S. Schumm, J. M. Tour, *Macromolecules* **1994**, *27*, 2348.

[93] N. Aratani, A. Takagi, Y. Yanagawa, T. Matsumoto, T. Kawai, S. Yoon Zin, D. Kim, A. Osuka, *Chem. – Eur. J.* **2005**, *11*, 3389.

[94] N. Aratani, A. Osuka, H. Kim Yong, H. Jeong Dae, D. Kim, *Angew. Chem., Int. Ed.* **2000**, *39*, 1458.

[95] F. P. V. Koch, M. Heeney, P. Smith, *J. Am. Chem. Soc.* **2013**, *135*, 13699.

[96] F. P. V. Koch, P. Smith, M. Heeney, *J. Am. Chem. Soc.* **2013**, *135*, 13695.

[97] K. Inouchi, S. Kobashi, K. Takimiya, Y. Aso, T. Otsubo, *Org. Lett.* **2002**, *4*, 2533.

[98] W. Ten Hoeve, H. Wynberg, E. E. Havinga, E. W. Meijer, *J. Am. Chem. Soc.* **1991**, *113*, 5887.

[99] Q. Wang, Y. Qu, H. Tian, Y. Geng, F. Wang, *Macromolecules* **2011**, *44*, 1256.

[100] S. Park, K. Kwon, D. Cho, B. Lee, M. Ree, T. Chang, *Macromolecules* **2003**, *36*, 4662.

[101] S. Park, D. Cho, J. Ryu, K. Kwon, W. Lee, T. Chang, *Macromolecules* **2002**, *35*, 5974.

[102] B. Chung, S. Park, T. Chang, *Macromolecules* **2005**, *38*, 6122.

[103] L. Groenendaal, H. W. I. Peerlings, J. L. J. van Dongen, E. E. Havinga, J. A. J. M. Vekemans, E. W. Meijer, *Macromolecules* **1995**, *28*, 116.

[104] J. Lawrence, S.-H. Lee, A. Abdilla, M. D. Nothling, J. M. Ren, A. S. Knight, C. Fleischmann, Y. Li, A. S. Abrams, B. V. K. J. Schmidt, M. C. Hawker, L. A. Connal, A. J. McGrath, P. G. Clark, W. R. Gutekunst, C. J. Hawker, *J. Am. Chem. Soc.* **2016**, *138*, 6306.

[105] J. Lawrence, E. Goto, J. M. Ren, B. McDearmon, D. S. Kim, Y. Ochiai, P. G. Clark, D. Laitar, T. Higashihara, C. J. Hawker, *J. Am. Chem. Soc.* **2017**, *139*, 13735.

[106] N. S. Vail, C. Stubbs, C. I. Biggs, M. I. Gibson, *ACS Macro Lett.* **2017**, *6*, 1001.

[107] Y. Hoshino, S. Shimohara, Y. Wada, M. Nakamoto, Y. Miura, *J. Mater. Chem. B* **2020**, *8*, 5597.

[108] Y. Hoshino, S. Taniguchi, H. Takimoto, S. Akashi, S. Katakami, Y. Yonamine, Y. Miura, *Angew. Chem., Int. Ed.* **2020**, *59*, 679.

[109] J. Vandenbergh, G. Reekmans, P. Adriaensens, T. Junkers, *Chem. Sci.* **2015**, *6*, 5753.

[110] J. Vandenbergh, G. Reekmans, P. Adriaensens, T. Junkers, *Chem. Commun.* **2013**, *49*, 10358.

[111] J. J. Haven, J. A. De Neve, T. Junkers, *ACS Macro Lett.* **2017**, *6*, 743.

[112] C. Zhang, M. W. Bates, Z. Geng, A. E. Levi, D. Vigil, S. M. Barbon, T. Loman, K. T. Delaney, G. H. Fredrickson, C. M. Bates, A. K. Whittaker, C. J. Hawker, *J. Am. Chem. Soc.* **2020**, *142*, 9843.

[113] M. T. Stone, J. M. Heemstra, J. S. Moore, *Acc. Chem. Res.* **2006**, *39*, 11.

[114] F. A. Leibfarth, J. A. Johnson, T. F. Jamison, *Proc. Nat. Acad. Sci.* **2015**, *112*, 10617.

[115] A. C. Wicker, F. A. Leibfarth, T. F. Jamison, *Polym. Chem.* **2017**, *8*, 5786.

[116] Y. Kim, H. Park, A. Abdilla, H. Yun, J. Han, G. E. Stein, C. J. Hawker, B. J. Kim, *Chem. Mater.* **2020**, *32*, 3597.

[117] B. A. G. Lamers, B. van Genabeek, J. Hennissen, B. F. M. de Waal, A. R. A. Palmans, E. W. Meijer, *Macromolecules* **2019**, *52*, 1200.

[118] J. J. Haven, J. De Neve, A. Castro Villavicencio, T. Junkers, *Polym. Chem.* **2019**, *10*, 6540.

[119] J. E. Báez, K. J. Shea, P. R. Dennison, A. Obregón-Herrera, J. Bonilla-Cruz, *Polym. Chem.* **2020**, *11*, 4228.

[120] Y. Xia, N. A. D. Burke, H. D. H. Stöver, *Macromolecules* **2006**, *39*, 2275.

[121] L. Leibler, *Macromolecules* **1980**, *13*, 1602.

[122] F. S. Bates, G. H. Fredrickson, *Annu. Rev. Phys. Chem.* **1990**, *41*, 525.

[123] G. Martínez-Rugerio, A. Arbe, J. Colmenero, A. Alegría, *Macromolecules* **2017**, *50*, 8688.

[124] B. Oschmann, J. Lawrence, M. W. Schulze, J. M. Ren, A. Anastasaki, Y. Luo, M. D. Nothling, C. W. Pester, K. T. Delaney, L. A. Connal, A. J. McGrath, P. G. Clark, C. M. Bates, C. J. Hawker, *ACS Macro Lett.* **2017**, *6*, 668.

[125] Y. Sun, R. Tan, Z. Ma, Z. Gan, G. Li, D. Zhou, Y. Shao, W.-B. Zhang, R. Zhang, X.-H. Dong, *ACS Cent. Sci.* **2020**, *6*, 1386.

[126] M. R. Golder, Y. Jiang, P. E. Teichen, H. V. T. Nguyen, W. Wang, N. Milos, S. A. Freedman, A. P. Willard, J. A. Johnson, *J. Am. Chem. Soc.* **2018**, *140*, 1596.

[127] J. Sun, A. A. Teran, X. Liao, N. P. Balsara, R. N. Zuckermann, *J. Am. Chem. Soc.* **2013**, *135*, 14119.

[128] J. Sun, X. Liao, A. M. Minor, N. P. Balsara, R. N. Zuckermann, *J. Am. Chem. Soc.* **2014**, *136*, 14990.

[129] J. Sun, X. Jiang, A. Siegmund, M. D. Connolly, K. H. Downing, N. P. Balsara, R. N. Zuckermann, *Macromolecules* **2016**, *49*, 3083.

[130] E. C. Davidson, A. M. Rosales, A. L. Patterson, B. Russ, B. Yu, R. N. Zuckermann, R. A. Segalman, *Macromolecules* **2018**, *51*, 2089.

[131] B. Yu, S. P. O. Danielsen, A. L. Patterson, E. C. Davidson, R. A. Segalman, *Macromolecules* **2019**, *52*, 2560.

[132] S. Thomas Tessy, W. Hwang, R. Sita Lawrence, *Angew. Chem., Int. Ed.* **2016**, *55*, 4683.

[133] S. R. Nowak, W. Hwang, L. R. Sita, *J. Am. Chem. Soc.* **2017**, *139*, 5281.
[134] C. Singh, M. Goulian, A. J. Liu, G. H. Fredrickson, *Macromolecules* **1994**, *27*, 2974.
[135] C. Tschierske, *J. Mater. Chem.* **1998**, *8*, 1485.
[136] Y.-L. Loo, R. A. Register, A. J. Ryan, *Macromolecules* **2002**, *35*, 2365.
[137] H.-A. Klok, J. F. Langenwalter, S. Lecommandoux, *Macromolecules* **2000**, *33*, 7819.
[138] H. Schlaad, B. Smarsly, M. Losik, *Macromolecules* **2004**, *37*, 2210.
[139] B. van Genabeek, B. F. M. de Waal, B. Ligt, A. R. A. Palmans, E. W. Meijer, *ACS Macro Lett.* **2017**, *6*, 674.
[140] B. van Genabeek, B. A. G. Lamers, B. F. M. de Waal, M. H. C. van Son, A. R. A. Palmans, E. W. Meijer, *J. Am. Chem. Soc.* **2017**, *139*, 14869.
[141] B. van Genabeek, B. F. M. de Waal, A. Palmans, E. W. Meijer, *Polym. Chem.* **2018**, *9*, 2746.
[142] J. Sun, A. A. Teran, X. Liao, N. P. Balsara, R. N. Zuckermann, *J. Am. Chem. Soc.* **2014**, *136*, 2070.
[143] W. Chen, B. Wunderlich, *Macromol. Chem. Phys.* **1999**, *200*, 283.
[144] T. Kato, *Science* **2002**, *295*, 2414.
[145] M. Lee, B.-K. Cho, Y.-G. Jang, W.-C. Zin, *J. Am. Chem. Soc.* **2000**, *122*, 7449.
[146] M. E. Neubert, S. S. Keast, C. C. Law, M. C. Lohman, J. C. Bhatt, *Liq. Cryst.* **2005**, *32*, 781.
[147] A. Facchetti, M. Mushrush, H. E. Katz, T. J. Marks, *Adv. Mater.* **2003**, *15*, 33.
[148] K. Nickmans, N. Murphy Jeffrey, B. de Waal, P. Leclère, J. Doise, R. Gronheid, J. Broer Dick, A. P. H. J. Schenning, *Adv. Mater.* **2016**, *28*, 10068.
[149] R. H. Zha, G. Vantomme, A. Berrocal José, R. Gosens, B. de Waal, S. Meskers, E. W. Meijer, *Adv. Funct. Mater.* **2017**, *28*, 1703952.
[150] J. A. Berrocal, R. H. Zha, B. F. M. de Waal, J. A. M. Lugger, M. Lutz, E. W. Meijer, *ACS Nano* **2017**, *11*, 3733.
[151] B. A. G. Lamers, R. Graf, B. F. M. de Waal, G. Vantomme, A. R. A. Palmans, E. W. Meijer, *J. Am. Chem. Soc.* **2019**, *141*, 15456.
[152] A. M. Liquori, G. Anzuino, V. M. Coiro, M. D'Alagni, P. De Santis, M. Savino, *Nature* **1965**, *206*, 358.
[153] J. M. Ren, J. Lawrence, A. S. Knight, A. Abdilla, R. B. Zerdan, A. E. Levi, B. Oschmann, W. R. Gutekunst, S.-H. Lee, Y. Li, A. J. McGrath, C. M. Bates, G. G. Qiao, C. J. Hawker, *J. Am. Chem. Soc.* **2018**, *140*, 1945.
[154] Q. Gan, X. Wang, B. Kauffmann, F. Rosu, Y. Ferrand, I. Huc, *Nat. Nanotechnol.* **2017**, *12*, 447.
[155] J. C. Nelson, J. G. Saven, J. S. Moore, P. G. Wolynes, *Science* **1997**, *277*, 1793.
[156] R. B. Prince, S. A. Barnes, J. S. Moore, *J. Am. Chem. Soc.* **2000**, *122*, 2758.
[157] M. Siauw, S. Hawkett Brian, S. Perrier, *J. Polym. Sci., Part A: Polym. Chem.* **2011**, *50*, 187.
[158] A. Lamprou, D. Xie, G. Storti, H. Wu, *Colloid Polym. Sci.* **2014**, *292*, 677.
[159] M. L. Hawkins, S. S. Schott, B. Grigoryan, M. A. Rufin, B. K. D. Ngo, L. Vanderwal, S. J. Stafslien, M. A. Grunlan, *Polym. Chem.* **2017**, *8*, 5239.
[160] C. Appiah, G. Woltersdorf, W. H. Binder, *Polym. Chem.* **2017**, *8*, 2752.
[161] A. S. Knight, J. Larsson, J. M. Ren, R. Bou Zerdan, S. Seguin, R. Vrahas, J. Liu, G. Ren, C. J. Hawker, *J. Am. Chem. Soc.* **2018**, *140*, 1409.
[162] I. Otsuka, K. Fuchise, S. Halila, S. Fort, K. Aissou, I. Pignot-Paintrand, Y. Chen, A. Narumi, T. Kakuchi, R. Borsali, *Langmuir* **2010**, *26*, 2325.
[163] G. L. Sternhagen, S. Gupta, Y. Zhang, V. John, G. J. Schneider, D. Zhang, *J. Am. Chem. Soc.* **2018**, *140*, 4100.
[164] A. Das, K. Petkau-Milroy, G. Klerks, B. van Genabeek, R. P. M. Lafleur, A. R. A. Palmans, E. W. Meijer, *ACS Macro Lett.* **2018**, *7*, 546.
[165] K. Petkau-Milroy, A. Ianiro, M. M. L. Ahn, J. R. Magana, M. E. J. Vleugels, B. A. G. Lamers, R. Tuinier, I. K. Voets, A. R. A. Palmans, E. W. Meijer, *ACS Macro Lett.* **2020**, *9*, 38.
[166] M. E. J. Vleugels, M. E. de Zwart, J. R. Magana, B. A. G. Lamers, I. K. Voets, E. W. Meijer, K. Petkau-Milroy, A. R. A. Palmans, *Polym. Chem.* **2020**, *11*, 7170.
[167] G. Maayan, M. D. Ward, K. Kirshenbaum, *Proc. Nat. Acad. Sci.* **2009**, *106*, 13679.
[168] P. Chandra, A. M. Jonas, A. E. Fernandes, *J. Am. Chem. Soc.* **2018**, *140*, 5179.
[169] C. Zhang, D. S. Kim, J. Lawrence, C. J. Hawker, A. K. Whittaker, *ACS Macro Lett.* **2018**, *7*, 921.
[170] O. Gidron, M. Bendikov, *Angew. Chem., Int. Ed.* **2014**, *53*, 2546.
[171] M. Liu, L. Yin, L. Wang, T. Miao, X. Cheng, Y. Wang, W. Zhang, X. Zhu, *Polym. Chem.* **2019**, *10*, 1806.
[172] J. Li, A. Terec, Y. Wang, H. Joshi, Y. Lu, H. Sun, M. C. Stuparu, *J. Am. Chem. Soc.* **2017**, *139*, 3089.
[173] D. Tao, C. Feng, Y. Cui, X. Yang, I. Manners, M. A. Winnik, X. Huang, *J. Am. Chem. Soc.* **2017**, *139*, 7136.
[174] S. Zhang, N. E. Bauer, I. Y. Kanal, W. You, G. R. Hutchison, T. Y. Meyer, *Macromolecules* **2017**, *50*, 151.
[175] J. Ahner, D. Pretzel, M. Enke, R. Geitner, S. Zechel, J. Popp, U. S. Schubert, M. D. Hager, *Chem. Mater.* **2018**, *30*, 2791.
[176] Y. Morisaki, K. Inoshita, Y. Chujo, *Chem. – Eur. J.* **2014**, *20*, 8386.
[177] K. Denise, P. B. Eric, B. Michel, C. Laurence, L. Jean-François, *Adv. Funct. Mater.* **2017**, *27*, 1604595.
[178] K. L. Bicker, J. Sun, J. J. Lavigne, P. R. Thompson, *ACS Comb. Sci.* **2011**, *13*, 232.

AUTHOR BIOGRAPHIES

Bas van Genabeek conducted his PhD research with professor Bert Meijer at the Eindhoven University of Technology. The work focused on the precision synthesis of discrete block co-oligomers and the study of the influence of (mono)dispersity on self-assembly. After obtaining his PhD degree in 2018, he became employed at CRO SyMO-Chem, where he currently is involved with the design and synthesis of

complex drug derivatives for a promising, novel drug delivery platform.

Brigitte A. G. Lamers studied Chemical Engineering at Eindhoven University of Technology with internships at Queens University Belfast and University of California Santa Barbara. During her master's, she focussed on the synthesis of discrete amorphous-crystalline block co-oligomers in the research group of prof. Dr. E. W. Meijer after which she graduated as chemical engineer. In 2017, she started her PhD in the group of prof. Dr. E. W. Meijer. Her research focusses on the structure-property relationships between molecular structure and property in functional nanomaterials using discrete block co-oligomers.

Craig J. Hawker, FRS is Clarke Professor and holds the Alan and Ruth Heeger Chair of Interdisciplinary Science at UCSB where he directs the California Nanosystems Institute and the Dow Materials Institute. He came to UCSB in 2004 after 11 years as a Research Staff Member at the IBM Almaden Research Center in San Jose, CA. Professor Hawker's research activities focus on synthetic polymer chemistry and nanotechnology, integrating fundamental studies with the development of nanostructured materials for advanced properties and functions in microelectronics and biotechnology.

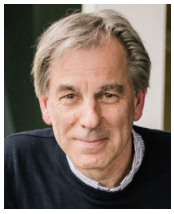

E.W. "Bert" Meijer is Distinguished University Professor and Professor of Organic Chemistry at the Institute for Complex Molecular Systems (ICMS) of the Eindhoven University of Technology, the Netherlands. After receiving his PhD degree in Organic Chemistry at the University of Groningen in 1982, he worked for 10 years in industry (Philips and DSM) on materials. In 1991 he was appointed in Eindhoven, while he has part-time positions in Nijmegen, Santa Barbara, and at the Max Planck Institute in Mainz.

Will R. Gutekunst received a BS in Chemistry from the University of Oklahoma in 2008 and a PhD in Organic Chemistry from the Scripps Research Institute under Prof. Phil S. Baran in 2013. Following a postdoctoral experience learning about polymer science in the laboratory of Prof. Craig J. Hawker at the University of California, Santa Barbara, Will started his independent career at the Georgia Institute of Technology in 2016. His lab is interested in the development of new methods for the synthesis of functional and renewable polymeric materials through the introduction of new concepts from organic chemistry.

Bernhard V. K. J. Schmidt completed his PhD in 2013 with Prof. Barner-Kowollik at the Karlsruhe Institute of Technology and a Post-Doc with Prof. Hawker at the University of California, Santa Barbara. Afterwards he joined the department of Prof. Antonietti at the Max Planck Institute of Colloids and Interfaces as a Group Leader. Recently, he was appointed as Lecturer in Synthetic Polymer Chemistry at the University of Glasgow. His research focusses on block copolymer self-assembly, metal–organic framework/polymer hybrids and carbon nitride/polymer hybrid materials.

How to cite this article: van Genabeek B, Lamers BAG, Hawker CJ, Meijer EW, Gutekunst WR, Schmidt BVKJ. Properties and applications of precision oligomer materials; where organic and polymer chemistry join forces. *J Polym Sci*. 2021;59:373–403. https://doi.org/10.1002/pol.20200862